2016

# Linking Obesity & Breast Cancer: Role Of Monocyte Chemoattractant Protein-1 And High Fat Diet-Induced Inflammation On Mammary Tumorigenesis

Taryn L. Cranford
*University of South Carolina*

# LINKING OBESITY & BREAST CANCER: ROLE OF MONOCYTE CHEMOATTRACTANT PROTEIN-1 AND HIGH FAT DIET-INDUCED INFLAMMATION ON MAMMARY TUMORIGENESIS

by

Taryn L. Cranford

Bachelor of Science
University of Tampa, 2012

---

Submitted in Partial Fulfillment of the Requirements

For the Degree of Doctor of Philosophy in

Biomedical Science

School of Medicine

University of South Carolina

2016

Accepted by:

E. Angela Murphy, Major Professor

Mitzi Nagarkatti, Chair, Examining Committee

Daping Fan, Committee Member

Udai Singh, Committee Member

Rebecca Bellone, Committee Member

Cheryl L. Addy, Vice Provost and Dean of the Graduate School

# DEDICATION

This work is dedicated to my family, the constant force in my life pushing me to always be better. To my little hummingbird, you are the joy in my life. I will never have a greater purpose in life than to be your mother. I hope if I am to teach you anything, it is that you little girl can do hard things. To my parents, you are all the good that is in me. You are my drive and inspiration to pursue cancer research. My pertinacious attributes could have only come from you and I still hear you both in the back of my mind telling me I can do anything. This has been a long journey but it wouldn't have been possible without both of you behind me.

# ACKNOWLEDGEMENTS

There are a few important people I would like to mention here and give a small token of appreciation for without whom I wouldn't have even attempted, let alone completed this journey.

I would like to thank my committee members, Drs. Angela Murphy, Mitzi Nagarkatti, Daping Fan, Udai Singh and Rebecca Bellone for their time and investment in me as a student and researcher. I would also like to acknowledge my NIH F31 NRSA Predoctoral Fellowship funding for supporting me and my research.

Dr. Angela Murphy, being a part of your research group these past few years has been a challenging but incredibly rewarding experience. You have inspired and encouraged me during some difficult and trying times and I truly appreciate your guidance and mentorship. It is incredibly challenging to be a hard working scientist and mother but somehow you make it look effortless. I really appreciate you and value everything I have learned from you.

Finally, Dr. Rebecca Bellone, you took a chance on me in your research group in 2011 and ended up changing my entire career path. You are the reason I fell in love with research and you have been the greatest academic driving force in my life. Words can neither qualify nor quantify what your guidance and friendship means to me. Thank you for everything.

# ABSTRACT

More than two-thirds of the adult population in the United States is classified as overweight or obese. In order to fully comprehend this rapidly increasing dilemma, further understanding of the complex phenomena that are involved with obesity and its many comorbidities is necessary. Chronic inflammation represents a distinctive, recurrent feature of obesity and has been associated with an increased risk of breast cancer. Monocyte chemoattractant protein 1 is a crucial component of the inflammatory process and represents a potential therapeutic treatment target, not only in obesity but also in breast cancer. Using a monocyte chemoattractant protein deficient model, we examined the role of this chemokine in the obesogenic inflammatory environment and results indicate that it can play a protective role in the development of adiposity and metabolic perturbations in a high fat diet-induced obesity murine model. Additionally, we examined the role of this chemokine in a model of triple negative breast cancer and report that deletion significantly reduces tumorigenesis and localized inflammation. Finally, we tested the central hypothesis that chronic inflammation plays a critical role in the progression and severity of obesity-induced hormone-dependent breast cancer and report significant proneoplastic effects. Further understanding of the etiopathogenesis of obesity and breast cancer has profound, prognostic effects. Therefore, continued research is required so that novel targeted therapies can be developed in this ever increasing portion of the population.

# TABLE OF CONTENTS

LIST OF FIGURES

# LIST OF ABBREVIATIONS

CCR2 ..... C-C Chemokine Receptor 2

C3 ..... C3(1)/SV40Tag

ER ..... Estrogen Receptor

H&E ..... Hematoxylin & Eosin

HFD ..... High Fat Diet

HP ..... Hormone Receptor Positive

IL ..... Interleukin

IκB ..... Inhibitor of NF-κB Kinase

IKK ..... IκK Kinase

IFG-1 ..... Insulin-like Growth Factor 1

IFN-γ ..... Interferon Gamma

ICAM-1 ..... Intercellular Adhesion Molecule 1

JNK ..... Jun Amino-terminal Kinase

LFD ..... Low Fat Diet

MAPK ..... Mitogen-activated Protein Kinase

MCP-1 ..... Monocyte Chemoattractant Protein 1

MIN ..... Mammary Intraepithelial Neoplasia

NF-κB ..... Nuclear Factor Kappa B

PDGF ..... Platelet Derived Growth Factor

PGE2 ..... Prostaglandin E2

PKC ..... Protein Kinase C

PyMT ..... PyMT/MMTV

TLR ..... Toll-like Receptor

TNF ..... Tumor Necrosis Factor

VCAM ..... Vascular Cellular Adhesion Molecule 1

VEGF ..... Vascular Endothelial Growth Factor

WT ..... Wild-type

# CHAPTER 1

# INTRODUCTION

Over one third of the adult population in the U.S. is obese, resulting in the continued rise in obesity-related conditions including heart disease, stroke, type-2 diabetes, non-alcoholic fatty liver disease and certain types of cancer (1-6). This global increase in body mass is an escalating society concern. Concomitant environmental factors such as sedentary lifestyle, poor diet choices, socioeconomic influences; and less frequently, genetic disorders involving metabolic outcomes and hormone secretion, result in weight gain. Although it is well known that obesity can be prevented through healthy dietary habits and physical activity (7, 8), interventions in a clinical setting have generally been unsuccessful, especially in the long-term (1, 9). Thus, changing behavior in this population has proven to be challenging. This has led to an explosion of studies to understand the pathways driving the pathologic processes associated with obesity so that therapeutic targets can be identified.

*1.1 Mechanisms of Obesity-Induced Inflammation and Insulin Resistance*

It is increasingly appreciated that the accumulation of inflammatory cells and other immune cell types in adipose tissue correlates with a continuing low grade inflammatory state that ultimately impairs adipocyte function and may contribute to the development of insulin resistance (5, 10-14). This immuno-metabolic axis modulates the dysfunctional responses characteristic of obesity including pro-inflammatory cytokine secretion, immune cell infiltration and disrupted function of tissues involved in glucose homeostasis, such as adipose tissue, liver and skeletal muscle (12). This obesogenic environment plays a critical role in the initiation of insulin resistance and altered glucose metabolism.

White adipose tissue, one of the two distinct forms of adipose tissue, is the depot most important to obesity and insulin resistance. It traditionally functions as lipid storage, storing triacylglycerides following energy excess and deploying these stored lipids during periods of energy deprivation (15). With obesity and insulin resistance there is an inapt spillover of triacylglyceride-derived free fatty acids due to the increases in lipolysis (16) and these free fatty acids can activate inflammatory pathways via toll-like receptors and impair insulin signaling. White adipose tissue is a multi-component organ composed primarily of adipocytes but can also act as an endocrine organ releasing cytokines and adipokines to include interleukin (IL)-6, IL-1β, tumor necrosis factor (TNF)-α, leptin and adiponectin (17). In the insulin resistant state, these inflammatory cytokines activate several serine kinases, including IκK kinase (IKK) and Jun amino-terminal kinases (JNK). These kinases promote the phosphorylation of serine residues of the insulin signaling pathway, which can inhibit insulin action (18). White adipose tissue is unique in its plasticity and can expand with increases in weight gain. This expansion is accompanied by changes in function of the adipose tissue to include cytokine and chemokine secretion, immune cell infiltration, hypoxia, cell death, as well as fatty acid metabolism and storage. Mature adipocytes secrete IL-6, monocyte chemoattractant protein 1 (MCP-1), leptin, and adiponectin in a regulatory manner, these adipokines and cytokines can act in a paracrine, endocrine or autocrine manner to regulate glucose and lipid homeostasis (19).

It seems increasingly probable, given the complexity of pro-inflammatory signaling pathways, that a combination of cytokine-induced stimuli would elicit greater effective activation of the inflammation/insulin resistance paradigm than a single entity

alone. It is known that IL-1, TNF-α, and toll-like receptor 4 (TLR4) converge at the inhibitor of NF-κB kinase complex (IκB kinase) (20) and that nuclear factor kappa B (NF-κB) and JNK mitogen-activated protein kinase (MAPK) pathways link obesity, inflammation, and insulin resistance(21). But what instigates and consequentially propagates this inflammation?

Reduced ability of the adipose tissue to support the increases in lipids and store excess fats and an increased hypoxic environment both contribute to the influx of inflammation that accompanies the obesity phenotype. Adipose tissue hypoxia is a metabolic stressor that is partially induced by inadequate blood supply reaching the expanding organ. Tissue inflammation is associated with regions of hypoxia and is also linked to NF-κB signaling (22). Decreased adipose tissue expandability, leading to free fatty acid spillover, results in elevated circulating free fatty acids. This results in enhanced lipid accumulation in peripheral tissues such as the liver and skeletal muscle, inducing morphological and metabolic alterations leading to an inflamed and insulin resistant state by various processes.

Inflammation is a crucial mediator in obesity-induced insulin resistance. The expansion of white adipose tissue with obesity and the corresponding influx of inflammatory cells, such as macrophages, initiate a cascade of inflammatory events that directly contribute to an altered glucose response and insulin signaling. Evidence suggests that the mechanisms driving this pathogenic environment of obese white adipose tissue are actually a combination of events converging that escalate this pro-inflammatory state.

*1.2 Monocyte Chemoattractant Protein 1*

One such component of this obesogenic environment is MCP-1. MCP-1 (CCL2) is a member of the C-C chemokine family that bind to G protein coupled receptors to regulate macrophage recruitment during wound healing, infection, and inflammation (23-25) and is the most extensively studied chemokine. MCP-1 was the first discovered human CC chemokine and is located on chromosome 17 (23). MCP-1 is a small, soluble chemokine 13kDa in size and shares high sequence homology with other members of the MCP family (MCP-1, 2, 3 and 4). MCP-1 is expressed in response to a cell stressor, such as oxidative stress, or growth factor but can also be constitutively expressed by a variety of cell types including epithelial, smooth muscle, endothelial, fibroblasts, mesangial, monocytic, astrocytic, and microglial cells (23, 26-28). However, the major source of MCP-1 are monocytes and macrophages and their activity is regulated by the secretion of various cytokines (29). In addition, adipocytes have been recognized as an important source of MCP-1 (30, 31).

MCP-1 modulates cell chemotaxis by binding to G-protein coupled receptors on the surface of migratory leukocytes that have been targeted for activation. Once the receptors have been activated, they trigger a well-defined intracellular signaling cascade that results in the formation of inositol triphosphate, intracellular calcium release and protein kinase C (PKC) activation (32). MCP-1 binds to the C-C chemokine receptor 2 (CCR2) receptor in target cells that is constitutively expressed in monocytes but only detectable in T cells after activation (33). Evidence suggests that serine/threonine kinases are required for MCP-1-stimulated chemotaxis (34), and various kinases have been implicated in MCP-1 signal transduction; including the MAP kinases ERK1 and ERK2,

Janus kinase JAK2, the stress activated kinases JNK1 and p38, phospholipase C and two isoforms of PI3-kinase (p85/p110 and C2α) (35-38). In addition to modulating chemotactic activity for leukocytes, studies have indicated that MCP-1 is multi-faceted and can also play a role in tumor metastasis and angiogenesis, the immune and vascular systems, as well as in modulation of cell proliferation, apoptosis, and protein synthesis (39).

MCP-1 expression is regulated at the transcriptional level by various inducers such as TNFα, interferon gamma (IFN-γ), platelet derived growth factor (PGDF) and stress factors (40). In many of these regulatory responses, the pro-inflammatory NF-κB transcription factor is a key mediator. The increase in NF-κB activity in response to these inducers is well correlated with mononuclear cell infiltration and expression of MCP-1 and adhesion molecules such as intercellular adhesion molecule-1 (ICAM-1) and vascular cellular adhesion molecule-1 (VCAM-1) (41).

MCP-1 has been shown to play a role in many disease pathologies and chronic expression of MCP-1 contributes to inflammatory diseases including obesity, rheumatoid arthritis, atherosclerosis, and fibrosis (42-45). Moreover, several studies have shown MCP-1 to be overexpressed in cancers of the breast and ovary and that increased expression of MCP-1 in tumor cells correlates with increases in macrophage infiltration and tumor vascularization (46-48).

*1.3 Monocyte Chemoattractant Protein 1 & Obesity*

Overnutrition causes cellular stress in hypertrophic adipocytes, resulting in the release of pro-inflammatory cytokines, free fatty acids and the macrophage-attracting

chemokine MCP-1 (49, 50). Clinical studies have documented elevated mRNA levels of MCP-1 and that of its receptor, CCR2, in the visceral adipose tissue and elevated MCP-1 protein levels in the layer of peritoneum that surrounds abdominal organs in obese subjects. Experimental studies in high fat diet-fed rodents have reported similar trends with increases in mRNA expression of MCP-1 and its receptor, CCR2, in visceral adipose tissue. For example, we have reported an increase in mRNA expression levels of MCP-1 (~8 fold) in epididymal adipose tissue of mice following 16 weeks of consumption of a high fat diet that was designed to be similar to the standard American diet (51). Consistent with experimental evidence, increased circulating levels of plasma MCP-1 are found in obese and type 2 diabetic patients, indicative of increased systemic levels of inflammation. MCP-1 is predominantly released by immune cells including macrophages, however, given its recent attention as an adipokine we now know that it is also produced by adipocytes themselves (52).

Although the tissues and cell types involved in obesity-induced inflammation are not fully understood, there is increasing interest in the role of adipose tissue macrophages in these inflammatory changes. Studies in both humans and rodents show increases in adipose tissue macrophage content correlate with increases in body weight and insulin resistance (14, 53, 54). Adipose tissue macrophage content is higher in the visceral fat than the subcutaneous fat in obese subjects and weight loss leads to a reduction in adipose tissue macrophage content (55). Adipose tissue macrophages provide a potential link between inflammation and insulin resistance as they are the prominent source of inflammatory cytokines such as TNF-α and IL-6, which can inhibit insulin action (54, 56).

While quantitative changes in adipose tissue macrophage content with obesity is well supported in the literature, very little is known about variations in function and how these are modified with the development of obesity. Macrophages are characterized by a remarkable degree of plasticity and show significant heterogeneity in regards to function. They are able to adapt to a variety of environmental cues and different stimuli activate macrophages to express distinct patterns of surface markers, chemokines and metabolic enzymes that ultimately generate the diversity of macrophage function seen in inflammatory and steady-state settings (57, 58). The classical view presents a highly simplified M1/M2 phenotype classification (59). M1 or "classically activated" macrophages possess the cell surface marker CD11c, secrete pro-inflammatory cytokines and contribute to the induction of insulin resistance (57). Conversely, M2 or "alternatively activated" macrophages, have a different gene expression profile characterized by the relatively high expression of surface marker CD206 and anti-inflammatory cytokine expression (60). M2 macrophages are believed to participate in the blockade of inflammatory responses and in the promotion of tissue repair (61). However, such a system ignores the innumerable variety of phenotypes and has since been replaced with an understanding of the diverse macrophage population and that macrophages are likely activated across a continuum of these states. In a high fat diet-induced obesogenic state, circulating $Ly6C^{+}$ inflammatory monocytes continuously infiltrate the adipose tissue in a MCP-1-dependent manner and differentiate into adipose tissue macrophages (62). Under the influence of environmental cues, free fatty acids, and inflammatory cytokines the recruited monocytes differentiate into pro-inflammatory adipose tissue macrophages initiating a vicious cycle of inflammation. This paracrine

loop is recapitulated by free fatty acids released from adipocytes and inflammatory mediators that elicit the production of even more inflammatory cytokines (such as IL-6, IL-1β, and TNFα) by the adipose tissue macrophages (63).

*1.4 Breast Cancer & Obesity*

Breast carcinomas continue to be the most commonly occurring cancer in women and the second leading cause of cancer-related deaths. Breast cancer incidence and mortality rates are rapidly increasing in Asian countries such as China and India as the adoption of a "western" lifestyle continues to increase (64). A 2010 meta-analysis of 43 studies found that obesity at diagnosis is associated with poorer breast cancer specific and overall survival (65) and links between obesity and an increased risk of breast cancer recurrence and shorter disease-free survival have also been established (66). Obesity is not only characterized by increases in the amount of adipose tissue but also changes in the adipose tissue biology. Multiple molecular changes arising as a consequence of increased amounts of body fat are likely to contribute to the increased incidence of neoplasia and worse outcomes in the obese population. These changes include increased inflammatory cell infiltration, hyperinsulinemia, adipokine imbalances, increased cytokine and estrogen levels, and elevating insulin-like growth factor 1 (IGF-1) levels. These proneoplastic changes are likely to contribute to the elevated cancer incidence in general and worse overall outcomes associated with obesity and breast cancer.

One integrating mechanism that links obesity and breast cancer risk is the role of chronic inflammation. Chronic inflammation is recognized as an important mediator in the clinical and biochemical complications associated with obesity and also breast tumor biology and causation. Inflammation in adipose tissue, with infiltration by macrophages,

is well known to occur with obesity and its presence in the breast creates local conditions that favor breast epithelial cell transformation, cancer cell proliferation and invasion as well as tumor-related neovascularization. Adipose tissue macrophages can comprise up to 40% of the cells in obese adipose tissue and histologically, this macrophage infiltration manifests as inflammatory foci known as crown-like structures (67). Initially identified in visceral fat, these inflammatory foci have recently been observed in breast white adipose tissue of obese women as the abundance of these crown-like structures generally increases proportionally with body mass (68).

Breast cancer is a uniquely heterogeneous disease with different biological and clinical patterns between younger and older women. Thus, menopausal status as a prognostic factor becomes a topic of scrutiny. In the case of younger women, the link between body mass and breast cancer risk is more controversial. Some clinical studies in premenopausal women report a null or inverse association of obesity and breast cancer risk (69-72), while other investigators report weight gain and central obesity increase the risk of premenopausal breast cancer (73-77). In postmenopausal women the relationship is clearer; the majority of evidence supports a direct link between high fat diet-induced obesity and the risk for certain clinical subtypes of breast cancer (78-95). The molecular heterogeneity of breast cancers is now well recognized, with at least five different subtypes identified through molecular profiling (96). With obesity, estrogen and progesterone hormone-dependent breast cancers are of importance as estrogen signaling is likely to be a key contributor to obesity-associated breast cancer. Importantly, activation of estrogen receptor (ER) $\alpha$-dependent gene expression, as a consequence of adipose inflammation has been observed in murine mammary fat pads and human breast

samples (68, 97, 98). Additionally, estrogen metabolites have been proposed to have carcinogenic effects independent of ER signaling (99).

The primary site for estrogen biosynthesis in premenopausal women is the ovary but other peripheral sources have increased relative importance in estrogen synthesis. Of which, the adipose tissue expresses the estrogen synthase cytochrome aromatase p450 (100, 101), which is encoded by the *Cyp19* gene, and contributes to estrogen synthesis. In postmenopausal women, obesity and associated inflammation have been shown to contribute to increased breast cancer risk as the adipose tissue is the primary source of estrogen synthesis due to increased aromatase expression (102-104). In support of this concept, studies link aromatase expression in inflamed adipose tissue of obese women with the upregulation of proinflammatory mediators, such as macrophages, as aromatase transcription can be induced by the interaction of TNFα and IL-1β with their receptors. Breast tissue from obese women and mice have correlated increased expression of TNFα and IL-1β with increases in aromatase and ERα target genes (68, 97, 98). Regardless of ER status, dietary-induced chronic inflammation in breast adipose tissue promotes a localized environment conducive to increased tumor cell proliferation and metastatic capacity, with enhanced tumor-related angiogenesis. Thus, it is likely that paracrine interactions between macrophages and other cells types operate on an inflammatory axis that results in elevated estrogen biosynthesis and expression, however, further delineation of this axis is required before treatment mechanisms can be established.

*1.5 Monocyte Chemoattractant Protein 1 & Breast Cancer*

Clinical literature implicates elevations in MCP-1 in the development and progression of tumorigenesis. The mechanisms linking MCP-1 to cancer has largely

been attributed to its role as a powerful monocyte and macrophage chemoattractant, thus demonstrating its increased ability to recruit macrophages to the tumor microenvironment. In mammary tumors, high levels of MCP-1 significantly correlate with increased tumor-associated macrophage accumulation and infiltration into the tumor environment that can facilitate tumor progression through macrophage-mediated angiogenesis (105) and through secretion of growth and survival factors (48).

Macrophages are key mediators in the connection between inflammation and cancer progression and have been shown to play an important role in the development of tumor-related inflammation and neovascularization. Tumor-associated macrophages have been reported to represent up to 50% of the tumor mass (106) and have been shown to possess features involved with proangiogenic capabilities such as the expression of vascular endothelial growth factor (VEGF) and basic fibroblast growth factor (107) as well as a potent source of MCP-1 (108), thus leading to continued macrophage recruitment and enhancement (109). Tumor-associated macrophages are also a source of potent immunosuppressive molecules, such as IL-10 and prostaglandin E2 (PGE2), that contribute to tumor evasion from immune surveillance (110). Vascular endothelial cells also express MCP-1 receptors, and the chemokine stimulates capillary tube formation *in vitro* and the entire process of neovascularization *in vivo*, activity that is independent of MCP-1 well known role of chemotaxis (109). Recent studies demonstrate that MCP-1 also signals breast cancer cells to regulate survival and invasion (111) as well as promote primary tumor growth (112).

Cancer-free breast epithelial cells lack expression of MCP-1, while expression is significantly elevated in both neoplastic and stromal cells within the breast tumor

microenvironment (108, 113-119). Of these stromal cell types, fibroblasts and macrophages have been reported to express the highest levels of MCP-1 (115, 117). Given this evidence, expression of MCP-1 appears to be an acquired feature gained during tumor development demonstrating its necessity to the establishment and development of the tumor. A number of studies have reported that MCP-1 is significantly correlated with high tumor grade and lymph node metastasis as well as being associated with low levels of differentiation and poor prognosis (115, 120-122).

Evidence indicates that MCP-1 regulates multiple mechanisms of breast cancer progression and has been shown to be a significant prognostic indicator for breast cancer prognosis (48). Thus, this demonstrates the value of MCP-1 as a potential therapeutic target in inflammatory and difficult-to-treat cancers such as triple negative breast cancers.

*1.6 Statement of Hypothesis & Aim*

Significant advances in understanding the highly complex role of obesity and immunometabolism have been made in recent years. However, additional research is needed to fully elucidate this obesity-inflammation-aromatase axis so that potential biomarker development and targeted inflammatory signaling treatments can be established.

In these current studies, we tested the central hypothesis that chronic inflammation plays a critical role in the progression and severity of obesity-induced insulin resistance and hormone-dependent breast cancer progression. Additionally, we examined the role of MCP-1 expression in an obesogenic inflammatory environment and furthermore, the association of this chemokine with mammary tumorigenesis.

Substantial evidence indicates that obesity is linked to a state of chronic low-grade inflammation. In our first study, we examined the association of MCP-1 expression and its role on macrophage recruitment in a model of high fat diet-induced obesity. To test this association, we used a genetic MCP-1 global deletion mouse model and examined the absence of MCP-1 on adiposity, cellular infiltration, inflammation, and metabolic dysfunction following high fat diet (HFD) feeding in mice. Contrary to what we hypothesized, and largely inconsistent with the previously reported findings, we found that MCP-1 depletion increased adiposity, resulted in exaggerated metabolic dysfunction, and exacerbated infiltration of inflammatory cells into adipose tissue following 16 weeks of HFD feedings; thus indicating a protective role of MCP-1 expression in the adipose tissue.

More than 40,000 women in the United States die each year of breast cancer. Thus identifying novel targets for breast cancer treatment is of upmost clinical importance. In our second study, we tested the hypothesis that MCP-1 is an important component in the progression of mammary tumorigenesis and acts to increase macrophage infiltration into the mammary gland and also via pro-inflammatory pathways. To test this hypothesis, we introduced a genetic global MCP-1 knockout onto a triple negative model of breast cancer and examined differences in tumorigenesis. MCP-1 deficiency significantly decreased mammary tumorigenesis and reduced inflammation in the mammary gland and tumor; thus, confirming a pro-tumorigenic role of this chemokine in this model.

More than two-thirds of breast cancer patients have tumors that express estrogen receptors and increased obesity results in elevated levels of estradiol. Consequently,

obese women are at a significantly increased risk of developing hormone receptor positive breast cancers. Our third study focuses on this increased risk and examines mammary tumorigenesis in response to high fat diet feedings in a transgenic murine model of tumorigenesis, an experimental model that presents morphological similarities with human breast cancer. Our results show that chronic consumption of a HFD increases mammary tumorigenesis and histopathological tumor stage progression in a premenopausal model of breast cancer.

Taken together, these studies demonstrate that inflammation has emerged as a leading player in obesity-related pathologies and cancer biology. Obesity provides a direct link between inflammation and dysregulated metabolism and not surprisingly, therefore has an emergent role in the etiopathogenesis of breast cancer. Given the profound clinical implications, more evidence is needed so that targeted therapies can be developed.

# CHAPTER 2

# ROLE OF MONOCYTE CHEMOATTRACTANT PROTEIN-1 ON INFLAMMATORY PROCESSES AND METABOLIC DYSFUNCTION FOLLOWING HIGH FAT DIET FEEDINGS IN THE FVB/N STRAIN[1]

[1] Cranford TL, Enos RT, Velazquez KT, McClellan JL, Davis JM, Singh UP, Nagarkatti M, Nagarkatti PS, Robinson CM, Murphy EA. Role of Monocyte Chemoattractant Protein-1 on inflammatory processes and metabolic dysfunction following high-fat diet feedings in the FVB/N strain, *Int J Obes,* (2016) May;40(5):844-51

*Abstract*

MCP-1 is known to be an important chemokine for macrophage recruitment. Thus, targeting MCP-1 may prevent the perturbations associated with macrophage-induced inflammation in adipose tissue. However, inconsistencies in the available animal literature have questioned the role of this chemokine in this process. The purpose of this study was to examine the role of MCP-1 on obesity-related pathologies. Wild-type (WT) and MCP-1 deficient mice on an FVB/N background were assigned to either low-fat-diet (LFD) or HFD treatment for a period of 16 weeks. Body weight and body composition were measured weekly and monthly, respectively. Fasting blood glucose and insulin, and glucose tolerance were measured at 16 weeks. Macrophages, inflammatory mediators, and markers of fibrosis were examined in the adipose tissue at sacrifice. As expected, HFD increased adiposity (body weight, fat mass, fat percent, and adipocyte size), metabolic dysfunction (impaired glucose metabolism and insulin resistance) macrophage number ($CD11b^{+}F480^{+}$ cells, and gene expression of EMR1 and CD11c), inflammatory mediators (pNFκB and pJNK, and mRNA expression of MCP-1, CCL5, CXCL14, TNF-α, and IL-6), and fibrosis (expression of IL-10, IL-13, TGF-β, and MMP2) ($P<0.05$). However, contrary to our hypothesis, MCP-1 deficiency exacerbated many of these responses resulting in a further increase in adiposity (body weight, fat mass, fat percent and adipocyte size), metabolic dysregulation, macrophage markers (EMR1), inflammatory cell infiltration, and fibrosis (formation of type I and III collagens, mRNA expression of IL-10 and MMP2) ($P<0.05$). These data suggest that MCP-1 is protective against weight gain, metabolic dysregulation, inflammatory cell infiltration, and fibrosis in the FVB/N strain in response to HFD feedings.

*2.1 Introduction*

Over one third of the adult population in the U.S. is obese, resulting in a rise in obesity-related conditions including heart disease, stroke, type-2 diabetes, and certain types of cancer (1-6). Although it is well known that obesity can be prevented through healthy dietary habits and physical activity (7, 8), interventions in a clinical setting have generally been unsuccessful, especially in the long-term (1, 9). Thus, changing behavior in this population has proven to be challenging. This has led to an explosion of studies to understand the pathways driving the pathologic processes associated with obesity so that therapeutic targets can be identified.

A pathophysiological mechanism that can link obesity to disease risk is chronic inflammation. Obesity-associated inflammation is largely mediated by quantitative and phenotypic changes in adipose tissue macrophages. Approximately 45-60% of adipose tissue cells express the F4/80 macrophage marker in obese mice, whereas only 10-15% of cells from lean mice express this marker (14). In addition, adipose tissue macrophages in obese mice exhibit a pro-inflammatory M1 phenotype, whereas those from lean mice have an anti-inflammatory M2 phenotype (61, 123). Emerging evidence also associates macrophages with the dysregulation of metabolic homeostasis given the recent reports implicating their role in leptin and insulin resistance (124, 125). Thus, targeting macrophage recruitment may reverse obesity-related pathologies.

As such, several studies have examined the role of chemokines for their ability to reduce macrophage infiltration in mouse models of diet-induced obesity. Monocyte chemoattractant protein 1 (MCP-1) is perhaps the most widely investigated chemokine in this regard. It is increased in white adipose tissue of obese subjects resulting in

recruitment of bone-derived monocytes, which infiltrate the tissue from circulation (126, 127). Recently, it has been reported that MCP-1 can even induce macrophage cell division in adipose tissue implants, whereas MCP-1 deficiency *in vivo* decreases adipose tissue macrophage proliferation (128). MCP-1 has also been implicated in playing a role in metabolism; mice engineered to express an MCP-1 transgene in adipose tissue are reported to be insulin resistant (129). However, while the majority of data supports a role for MCP-1 on high-fat-diet (HFD) related pathologies there have been some inconsistencies, at least in the animal literature. For example, Inouye *et al*., reported no change in adipose tissue macrophage number in MCP-1 deficient mice following diet-induced obesity but in fact showed that these mice gained more weight, were glucose intolerant, had mildly increased plasma glucose and were hyperinsulinemic compared with wild-type mice suggesting a beneficial effect of this chemokine on metabolism independent of its macrophage recruiting abilities (130). While the inconsistences in the literature are still largely unexplained, Galastri *et al*., reported that lack of MCP-1 differently affects inflammation according to the genetic background in a model of diet-induced steatohepatitis (131).

We sought to examine the role of MCP-1 on adiposity, cellular infiltration, inflammation, and metabolic dysfunction following HFD feeding in mice. This was done using MCP-1 deficient mice on an FVB/N background, a model that was generated in our laboratory. The HFD was designed by our research team and has previously been reported to induce obesity and increase adipose tissue macrophage infiltration following 16 weeks of feedings (51, 132), albeit in the C57BL/6 strain. As expected, we confirmed an increase in adiposity, metabolic dysfunction, macrophage markers, and inflammation

with HFD feedings. However, contrary to what we hypothesized, our findings indicate that MCP-1 deficiency exacerbates many of these responses implicating a beneficial effect of this chemokine in HFD-related pathologies.

## *2.2 Materials & Methods*

### Animals

MCP1$^{-/-}$ mice on the C57BL/6 background and FVB/N wild-type mice were originally obtained from Jackson Laboratories (Bar Harbor, ME). The FVB/N mice were crossed with the C57BL/6 MCP1$^{-/-}$ strain, and then back-crossed an additional eight times to derive the FVB/N MCP1$^{-/-}$ strain. All experimental mice were bred and cared for in the animal research facility at the University of South Carolina. Male mice were used in all experiments and were genotyped for MCP-1 using the primer sequences as follows: mutant GCCAGAGGCCACTTGTGTAG, wild type forward TGACAGTCCCCAGAGTCACA and common TCATTGGGATCATCTTGCTG. They were housed, 3-5/cage, maintained on a 12:12-h light-dark cycle in a low stress environment (22°C, 50% humidity, low noise) and given food and water *ad libitum*. Principles of laboratory animal care were followed, and the Institutional Animal Care and Usage Committee of the University of South Carolina approved all experiments.

### Diets

At four weeks of age, wild-type and MCP-1$^{-/-}$ mice were randomly assigned to either a low-fat-diet (LFD) (n= 7 WT Con, n=7 MCP Con) or a HFD treatment (n=7 WT HFD, n=8 MCP HFD). The AIN-76A diet was used for the LFD. The HFD was designed by our laboratory and closely mimics the standard American diet (40% and 12%

of calories from total fat and saturated fat, respectively) (Bioserv, Frenchtown, NJ) (51, 133). Both diets contained similar vitamin and mineral content. Mice were fed their respective diets for 16 weeks.

Body weights, food intake, and body composition

Body weight and food intake were monitored weekly. Body composition was assessed approximately every 4 weeks (age 4, 9, 12, 16, and 20 weeks). Briefly, mice were placed under anesthesia (isoflurane inhalation) and were assessed for lean mass, fat mass, and body fat percentage via dual-energy x-ray absorptiometry (DEXA) (Lunar PIXImus, Madison, WI) (51).

Metabolism

Blood samples were collected from the tail vein after a 5-hour fast during week 16 of dietary treatment. Blood glucose concentrations were determined in whole blood using a glucometer (Bayer Contour, Michawaka IN). Insulin concentrations were determined in plasma using an ELISA kit (Mercodia, Uppsala, Sweden). Insulin resistance was estimated by the homeostatic model assessment (HOMA) index as follows: insulin resistance index = fasting insulin (μU/mL) x fasting glucose (mmol/L)/22.5 (134). Glucose tolerance tests were performed after 16 weeks of dietary treatment on mice fasted for 5 hours. Glucose (1g/kg) was given intraperitoneally and the blood glucose concentrations were measured intermittingly (0, 15, 30, 60, 90, and 120 minutes) over a two-hour period. Area under the curve (AUC) was calculated using the trapezoidal rule.

Tissue collection

Following 16 weeks of dietary treatment, mice were sacrificed for tissue collection. Epididymal, mesentery, and retroperitoneal fat pads as well as the liver were removed, weighed, and immediately snap-frozen in liquid nitrogen and stored at -80°C or fixed in 10% formalin.

Immunohistochemistry

A portion of epididymal adipose tissue was excised from each mouse, fixed overnight in 10% formalin, dehydrated with alcohol, and embedded in wax. Paraffin sections were stained with hematoxylin and eosin (H&E). Tissue content of type I and III collagens was examined using the picro-sirius red stain kit (Abcam, Cambridge, MA, USA, #150681).

Adipose tissue morphometry

To determine adipocyte size, the surface area of 100 adipocytes were determined (manual trace) from H&E stained slides using ImageJ software (National Institutes of Health, Bethesda, MD) (135) and then averaged to represent mean adipocyte size for each mouse.

Western blots

Epididymal adipose tissue was homogenized in Mueller buffer, which included a protease inhibitor cocktail (Sigma), 1% glycerophophate (100mM), 0.5% sodium orthovanadate (5mM) and 1% sodium fluoride (25mM) (51). The protein concentration was determined using the Bradford method (136). Proteins were fractioned onto Criterion precast gels (Bio-Rad, Hercules, CA) and were subsequently transferred to a polyvinylidene difluoride membrane overnight. Membranes were stained with a Ponceau

S solution to verify equal protein loading and transfer efficiency. Western blot analysis was performed as previously described using primary antibodies for phosphorylated (Ser536) and total NFκB p65 (#3033S) as well as phosphorylated (Thr183/Tyr185) and total JNK (#4671S) (Cell Signaling, Danvers, MA) (137, 138).

Magnetic cell sorting & flow cytometry

Epididymal adipose tissue samples were digested using Collagenase Type II (1mg/mL) and cRPMI (RPMI, 1% pentastrep, 1% BSA), strained, and centrifuged. Following lysing, cells were resuspended and centrifuged twice in FACS buffer to create a single cell suspension. Cells were counted and the cell volume of each sample was computed prior to pooling samples into each of the four treatment groups. An isolation buffer (PBS supplemented with 0.5% BSA and 2 mM EDTA) was used to resuspend the cells and CD11b MACS microbeads (Miltenyi Biotec Inc., San Diego, CA, #130-049-601) were used according to manufacturer's instruction. Cells were separated by magnetic properties in the column matrix (MACS, Auburn, CA, #130-042-201) and then resuspended in flow buffer. CD11b positive cells were counted using trypan blue. CD11b cells were stained for $F480^{+}$ (EBioscience, San Diego, CA, USA) and analyzed using a FC 500 (Beckman Coulter, Brea, CA) flow cytometer.

Real-time quantitative PCR

Epididymal adipose tissue was homogenized under liquid nitrogen using a polytron, and total RNA was extracted using TRIzol reagent (Invitrogen, Carlsbad, CA) and chloroform/isopropyl alcohol extraction. Murine 18s rRNA was used as the housekeeping gene to normalize all of the data obtained. Quantification of epididymal adipose tissue mRNA gene expression for macrophage markers (F4/80, CD11c, CD206),

cytokines (interleukin-6 (IL6), tumor necrosis factor α (TNFα), interleukin-10 (IL10), and interleukin-13 (IL13)), cell proliferation and differentiation cytokine transforming growth factor β (TGFβ), chemokines (MCP-1, C-X-C motif chemokine-12 (CXCL12), C-X-C motif chemokine-14 (CXCL14), C-C motif ligand-5 (CCL5), and fetuin-A), and matrix metalloproteinases (matrix metalloproteinase-2 (MMP2), matrix metalloproteinase-9 (MMP9)), (Applied Biosystems, Foster City, CA) were performed as previously described (138). Quantitative reverse transcriptase polymerase chain reaction analysis was carried out as per the manufacturer's instructions using TaqMan Gene Expression Assays (Applied Biosystems, Foster City, CA). Quantification of mRNA expression of all target genes was calculated using the $2\Delta\Delta C_T$ method.

Statistical analysis

All data were analyzed using commercial software (GraphPad Software, Prism 6, La Jolla, CA, USA). Total body weight, body weight percent change, body composition measurements and the glucose tolerance test were analyzed using a two-way analysis of variance at each time point. All other data were analyzed using a two-way analysis of variance. Bonferroni correction was used for all post-hoc analyses. Statistical significance was set with an α value of $P \leq 0.05$. Data are represented as mean ± SEM.

*2.3 Results*

FVB/N MCP1$^{-/-}$ mice fed a HFD have increased body weight gain and larger adipocyte size compared to wild-type mice fed the same diet

As expected, the HFD treatment increased body weight beginning at 1 week following initiation of the HFD treatment and remained elevated through the 16-week

treatment period (Figures 2.1A & 2.1B; P<0.05). Main effects of genotype were also observed; interestingly, MCP-1 deficient mice that weighed less than WT mice at baseline (4 weeks of age) were heavier at 7-12 weeks of HFD treatment (P<0.05; Figure 2.1A). Percent change in body weight is presented to reflect relative changes wherein MCP-1 deficient mice experienced greater weight gain from 1-16 weeks of age (P<0.05; Figure 2.1B). A significant interaction was observed for body weight at weeks 9-12 and weeks 10-11 for total body weight and body weight percent change, respectively (P<0.05); MCP-1 deficient mice increased body weight only when fed a HFD.

Similar effects were seen for the body composition analysis. A main effect of diet was seen at 4, 9, 12 and 16 weeks for both body fat (Figure 2.1C) and body fat percent (Figure 2.1D) (P<0.05), and a main effect of genotype was observed at 9 and 12 weeks for both of these outcomes (P<0.05). A significant interaction was found at 9 and 12 weeks for both total body fat and body fat percent (P<0.05); the observed increase with MCP-1 deficiency was dependent on diet treatment. For lean weight, only a main effect of diet was observed at 12 weeks (Figure 2.1E) (P<0.05).

The HFD treatment increased mean adipocyte size regardless of genotype (Figure 2.1F) (P<0.05). Further, a significant interaction was found as MCP-1 deficient mice fed a HFD had a significantly larger mean adipocyte size than the wild-type HFD-fed mice (P<0.05).

Visceral fat depots (epididymal, kidney, mesenteric) and liver were collected at sacrifice and weighed (Table 1). The HFD treatment increased mass in all fat depots as well as the liver ($P \leq 0.05$). Further, there was a main effect of genotype for the kidney fat weight and liver weight ($P \leq 0.05$); both were heavier in MCP-1 deficient mice.

In general, there were no differences among HFD-fed mice in weekly food intake (food consumed by mice in each cage/number of mice in cage) over the course of the study.

The absence of MCP-1 in FVB/N mice fed a HFD increases insulin resistance and aggravates glucose metabolism

HFD increased fasting blood glucose (Figure 2.2A) and insulin concentrations, (Figure 2.2B) as well as the HOMA index (Figure 2.2C) ($P \leq 0.05$). In addition, a main effect for genotype was observed where MCP-1 deficiency increased fasting blood insulin concentration and the HOMA index ($P<0.05$). Post-hoc analyses revealed that this effect occurred within the HFD groups only ($P \leq 0.05$). A glucose tolerance test (Figure 2.2D, E) revealed a main effect of diet (0, 15, 30, 60, 90 and 120 min) and genotype (15 and 30 min). Further, an interaction was found where MCP-1 deficient mice within the HFD treatment displayed poorer glucose metabolism than the wild-type mice at 30, 60, 90 and 120 minutes post-glucose administration ($P \leq 0.05$). Consistent with the aforementioned results, the AUC also revealed a main effect of diet and a significant interaction between the HFD treatment groups ($P \leq 0.05$).

Adipose tissue inflammatory cell infiltration is influenced by HFD consumption and the absence of MCP-1 in the FVB/N strain

H&E staining revealed increased inflammatory cell infiltration into epididymal fat (Figure 2.3A). Interestingly however, MCP-1 deficiency exacerbated this response as there was a further increase in the MCP1$^{-/-}$ HFD group.

These findings were confirmed using flow cytometric analysis (Figure 2.3B); we report an increase in CD11b$^{+}$F480$^{+}$ cells in HFD treated mice (78.7 and 89.8% for HFD

groups versus 22.6 and 27.6% for LFD groups). Again, this effect appeared to be worsened with MCP-1$^{-/-}$ within HFD as a further increase in CD11b$^{+}$F480$^{+}$ cells was observed (89.8% versus 78.7%).

RT-qPCR was performed to determine macrophage marker gene expression (Figure 2.3C**).** A significant main effect of diet was observed across all 3 markers where HFD treatment increased EMR1 (overall macrophage), CD11c (M1) and CD206 (M2) expression ($P<0.05$). A main effect of genotype was significant for EMR1 only; consistent with the IHC and FACS data, MCP-1 deficiency increased expression of EMR1 and post-hoc analyses revealed that this can attributed to an elevation within the HFD treatment only ($P<0.05$).

Long-term HFD feeding leads to adipose tissue inflammation but this is not significantly influenced by MCP-1 in the FVB/N strain

Western blot analysis revealed a main effect of diet on pNFκB (p65) and pJNK inflammatory pathway activation ($P<0.05$) (Figure 2.4A-B**)**. Gene expression of the chemokines MCP-1, CCL5 (Rantes) and CXCL14 were increased with HFD ($P<0.05$) and there was a trend for an increase in Fetuin A ($P=0.09$). Although there was no main effect of diet for CXCL12, there was a significant interaction where the effect of HFD was dependent on MCP-1 deficiency ($P<0.05$). The pro-inflammatory cytokines TNF-α and IL-6 were significantly upregulated in the HFD groups ($P<0.05$) (Figure 2.4C) but there was no effect of genotype and no interactions.

Prolonged HFD feedings leads to the formation of fibrosis in the adipose tissue of MCP-1 deficient mice on the FVB/N background

A main effect of diet was found across all 3 cytokine markers of fibrosis and tissue remodeling including IL-10, IL-13 and TGF-β ($P<0.05$). A main effect of genotype was observed for IL-10 ($P<0.05$) as well as a significant interaction between the wild-type HFD-fed mice and the MCP-1 deficient mice fed the same diet ($P<0.05$). There was a main effect of diet for both MMP2 and MMP9 ($P<0.05$); the mice treated with the HFD had significant increases in mRNA expression levels of MMP2, and conversely, decreases in mRNA expression levels of MMP9 ($P<0.05$) (Figure 2.5A). Further, for MMP2 there was a main effect of genotype ($P<0.05$) and also an interaction; MMP2 was increased in the MCP-1 deficient mice fed a HFD compared to the wild-type group fed the same diet. Picro-sirius red staining of the epididymal adipose tissue exhibited a substantial increase in the formation of type I and III collagens in the $MCP1^{-/-}$ HFD-fed mice (Figure 2.5B).

*2.4 Discussion*

Adipose tissue macrophages have been implicated in playing a role in obesity-related perturbations given their propensity to promote inflammation. MCP-1 is known to be an important chemokine for macrophage recruitment in various tissues. Thus, targeting this chemokine may prevent macrophage accumulation and subsequent inflammation in adipose tissue. While several studies have examined the role of MCP-1 on inflammatory processes in mouse models of obesity, the findings remain ambiguous. Given this, we sought to examine the importance of MCP-1 on HFD-related pathologies

using MCP-1 deficient mice on an FVB/N background. As expected, we found an increase in fat mass, metabolic dysfunction, macrophage markers, and inflammatory processes with HFD feedings. However, contrary to what we hypothesized, our findings indicate that MCP-1 deficiency increases adiposity, metabolic dysregulation, inflammatory cell infiltration, and fibrosis, implicating a potential protective effect of this chemokine in HFD-related pathologies in this mouse model.

The consequences of HFD feedings has been well characterized in the literature. In fact, we have reported that the exact HFD used in the current study leads to increased adiposity, macrophage accumulation and inflammation following 16 weeks of treatment (51, 137). However, the aforementioned studies were conducted in the C57BL/6 strain whereas in the current investigation we used mice on the FVB/N background; a strain that is often implicated as being resistant to diet-induced obesity (139-141). For example, studies have reported that HFD-feedings using a diet that consisted of 40% or higher fat content, for a period of 8 weeks, resulted in no changes in bodyweight or adiposity measurements (139-141). Montgomery *et al*., performed a similar feeding schedule for 8 weeks and concluded that there are only marginal changes in bodyweight and adiposity in FVB/N mice (142). However, not all the results have pointed towards resistance to diet-induced obesity in the FVB/N strain. For example, Metlakunta el al., reported increases in body weight, plasma insulin levels and fat pad weights in FVB/N mice fed a HFD for 19 weeks (143). The literature undoubtedly implicates strain-dependent differences in obesity and related outcomes in response to HFD feedings (142). However, the inconsistences that have been reported within the FVB/N strain, as well as others, may be due to the duration of HFD feedings, fat content of the diet, sex of

the mice, housing conditions, and/or differences in gut microbiota. For example, we have previously reported stark differences in adiposity, macrophage accumulation, and metabolic outcomes when the content of saturated fat, but not total fat, is altered (51). Nonetheless, our findings clearly confirm an increase in adiposity, metabolic dysfunction, macrophage accumulation, and inflammation following 16 weeks on a 40% HFD in the FVB/N strain.

MCP-1 is strongly linked to macrophage accumulation into adipose tissue and subsequent inflammation (124, 144). However, inconsistences in mechanistic studies in mice have questioned the role of this chemokine in this process. While the majority of the literature supports an influence of MCP-1 on macrophage recruitment and inflammatory processes in response to HFD feedings, several studies have reported no effect of MCP-1 and some have even reported that MCP-1 depletion leads to negative perturbations. Kanda *et al*., used both MCP-1 overexpression and depletion techniques in genetically obese and diet-induced obese mice and reported that MCP-1 does, in fact, contribute to macrophage infiltration and insulin resistance (144). These findings were consistent with Kamei *et al*. who reported an increase in macrophage accumulation and insulin resistance following MCP-1 overexpression in adipose tissue (129). Others have extended these findings using manipulation of the MCP-1 receptor (C-C motif chemokine receptor-2 (CCR2) (145). Despite these convincing investigations, several studies have reported no change in adipose tissue macrophage accumulation or insulin resistance in mouse models of obesity following interruption of MCP-1 (146-148). We generated an MCP-1 deficient FVB/N mouse in our lab and were thus interested in furthering the understanding of this chemokine in obesity-related pathologies given the inconsistencies

in the current literature. Contrary to what we hypothesized, and largely inconsistent with the previously reported findings, we found that MCP-1 depletion increased adiposity, resulted in exaggerated metabolic dysfunction, and exacerbated infiltration of inflammatory cells into adipose tissue following 16 weeks of HFD feedings. Adipocyte expansion and sustained inflammation are linked to fibrosis (149). Thus, given the increase in adipocyte hypertrophy and cell infiltration in MCP-1 deficient mice, we also measured fibrosis and report a substantial increase in collagens type 1 and III along with gene expression of select genes likely involved in this process including IL-10 and MMP2.

It is most likely that the exaggerated increase in metabolic dysfunction, inflammatory cell infiltration, and fibrosis in the MCP-1 deficient mice occurred in response to the earlier and more dramatic weight gain following HFD feedings in this strain. Based on the body composition data, the MCP-1 deficient mice clearly show an increase in total body fat and body fat percent at 9 weeks and 12 weeks of HFD feedings, which was no longer significantly different from the wild-type mice at 16 weeks. Thus, if adiposity is accelerated in MCP-1 deficient mice it seems intuitive that we would expect subsequent hastening of metabolic dysregulation, immune cell infiltration, and fibrosis. What is causing this increase in adiposity in the MCP-1 deficient mice is not clear. It is possible that MCP-1 may be involved in the regulation of adipogenesis, although there is limited literature to support such a hypothesis. A recent study however, reported that MCP-1 induced protein (MCP1P) induces adipogenesis resulting in an increase in the number of adipocytes (150). Based on this, it is plausible that a deficiency in MCP-1 would decrease adipocyte renewal resulting in hypertrophy of the existing

adipocytes and an ensuing unfavorable response as observed here. Our findings are supported by Inouye *et al*., who reported that depletion of MCP-1 resulted in more weight gain, glucose intolerance, increased plasma glucose, decreased serum adiponectin, and hyperinsulinemia compared with wild-type mice, although there were no differences in adipose tissue macrophage infiltration (130). Similarly, Kirk *et al*., using a similar MCP-1 knockout approach, reported higher levels of a macrophage-specific protein in multiple fat depots as well as increased adipose tissue weight in MCP-1 deficient mice (148).

A limitation of our study is that we examined only one time-point for the majority of outcomes; our data is limited to the 16-week time-point – a time-point when there were no differences in body composition, although differences in percent change of body weight were still evident. It would have been informative to have measured the influence of MCP-1 on inflammation and fibrosis at earlier time-points when much larger differences in body composition were observed to fully evaluate the role of this chemokine in obesity progression. It is certainly possible that differences in inflammatory mediators, chemokines, and possibly other parameters, between the groups would have been detected and/or greater had we measured these outcomes at earlier time-points.

Our data clearly suggest a necessary role for this chemokine in preventing obesity-related pathologies, at least in the FVB/N strain. However, given the previous literature, which is largely confined to the C57BL/6 strain, we performed an additional study using the C57BL/6 background utilizing the exact same diet and feeding duration. Although our sample size was limited (n=4-6/group), in general, we observed either no change or a slightly beneficial effect of MCP-1 depletion on adiposity and inflammation

following HFD feedings (Figure 2.6). This led us to conclude that lack of MCP-1 can differentially affect adiposity, metabolic processes, and inflammatory cell recruitment according to the genetic background. In support of this hypothesis, Galastri *et al*., reported similar strain differences in a mouse model of steatohepatitis in which the effects of MCP-1 deficiency were markedly different between mice on a C57BL/6 background and those on a Balb/C background (131).

In summary, we report for the first time that MCP-1 is protective against weight gain, metabolic dysregulation, inflammatory cell infiltration, and fibrosis in the FVB/N strain in response to HFD feedings. Although MCP-1 is clearly linked to adiposity and macrophage accumulation, the mechanistic studies that have evaluated this chemokine remain ambiguous. Future investigations incorporating multiple mouse strains, and examining several time-points of obesity development are necessary to understand the role of this chemokine on obesity-related pathologies in order to truly evaluate the therapeutic potential of MCP-1.

*2.5 Figures & Legends*

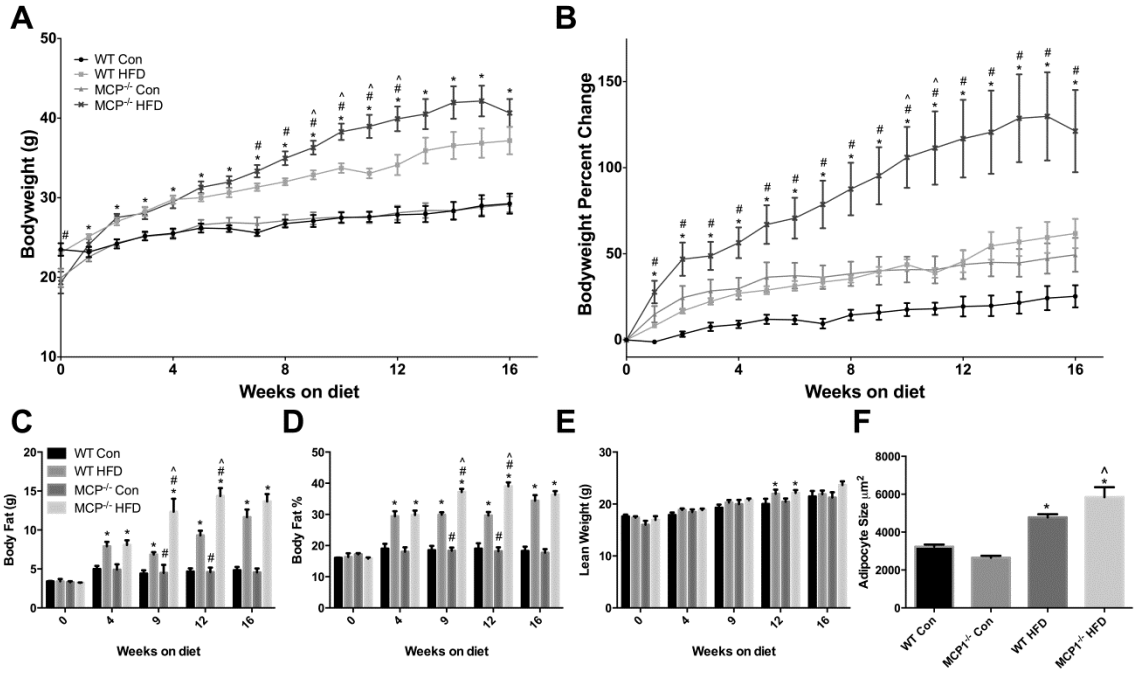


Figure 2.1:

Body weight characteristics. A. Body weight in grams. B. Body weight represented as percent change from starting weight. C. Body composition analysis, Body fat in grams. D. Body fat percentage. E. Lean weight in grams. F. Mean adipocyte size. *main effect of diet, #main effect of genotype. ^interaction between HFD groups. Data are represented as ± SEM and representative of two individual experiments, n=7 WT Con, n=7 WT HFD, n=7 MCP Con, n=8 MCP HFD.

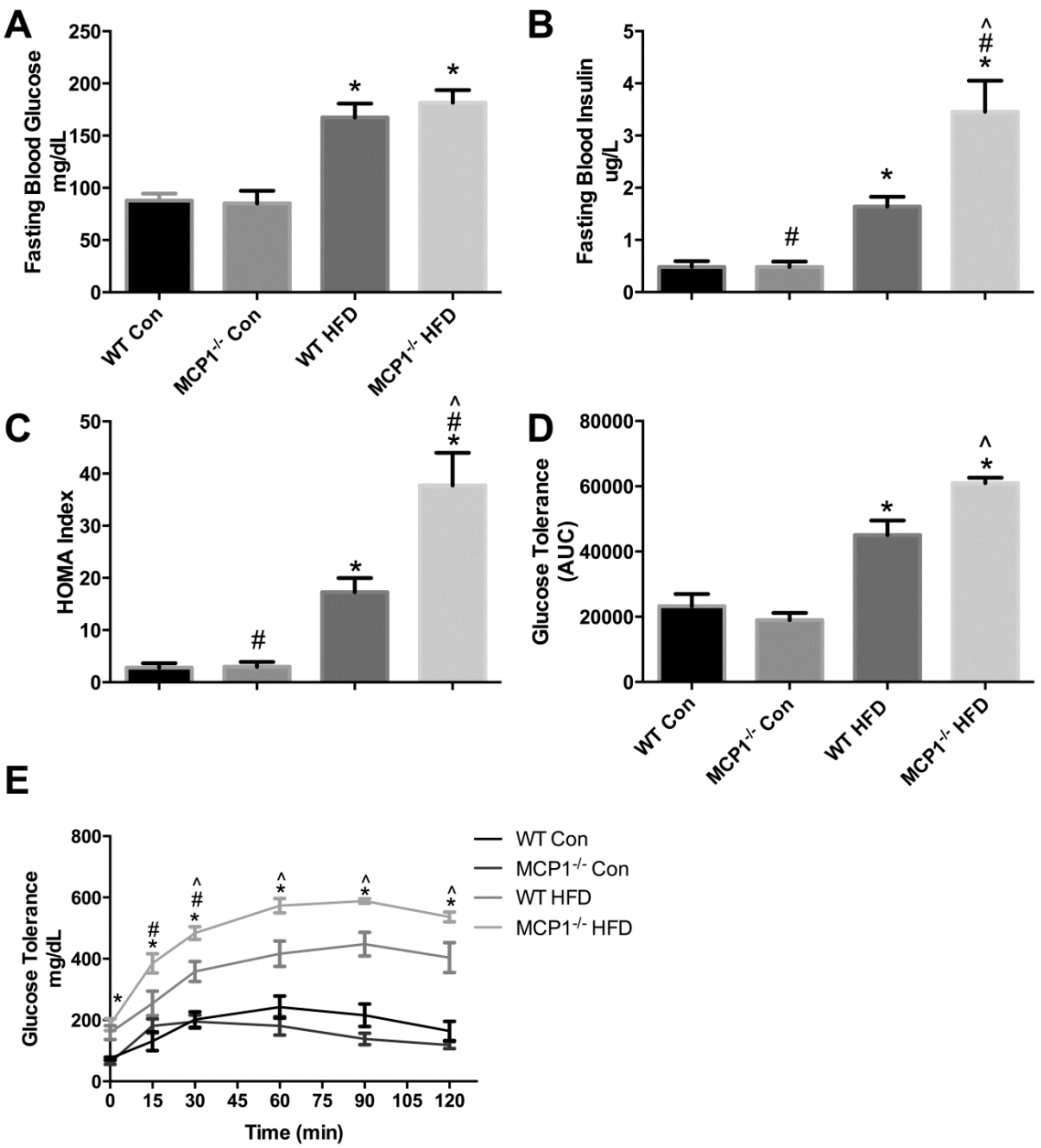


Figure 2.2:

Metabolic outcomes. A. Fasting blood glucose concentration (mg/dL). B. Fasting blood insulin concentration (ug/L). C. HOMA Index (n=7 WT Con, n=7 WT HFD, n=7 MCP Con, n=8 MCP HFD). D-E. Glucose tolerance test performed at 16 weeks of diet treatment (n= 4 WT Con, n=5 WT HFD, n=4 MCP Con, n=5 MCP HFD). *main effect of diet, #main effect of genotype. ^interaction between HFD groups. Data are represented as ± SEM and representative of two individual experiments.

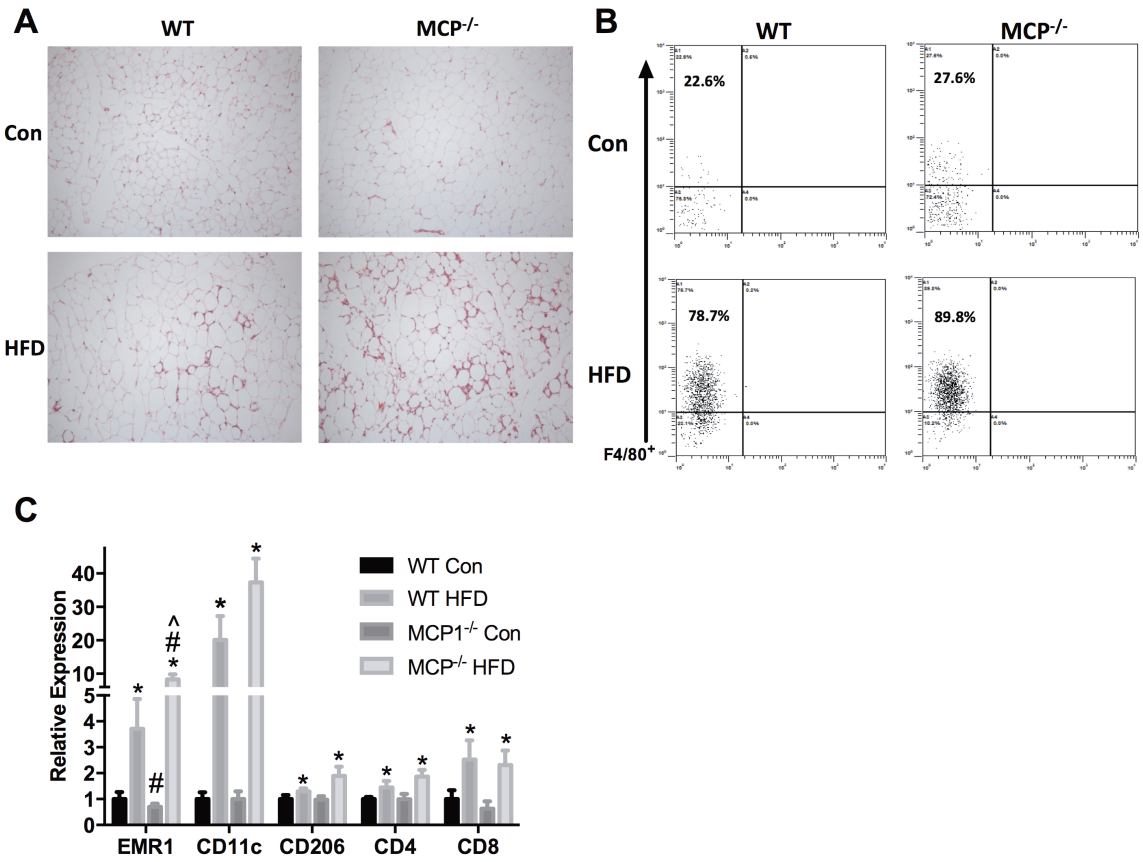


Figure 2.3:

Inflammatory cell population. A. Epididymal fat H&E staining. B. Flow cytometric analysis of $CD11b^{+}F480^{+}$ cells. C. Relative gene expression of macrophage markers in epididymal fat. *main effect of diet, #main effect of genotype. ^interaction between HFD groups. Data are represented as ± SEM and representative of two individual experiments, n=7 WT Con, n=7 WT HFD, n=7 MCP Con, n=8 MCP HFD.

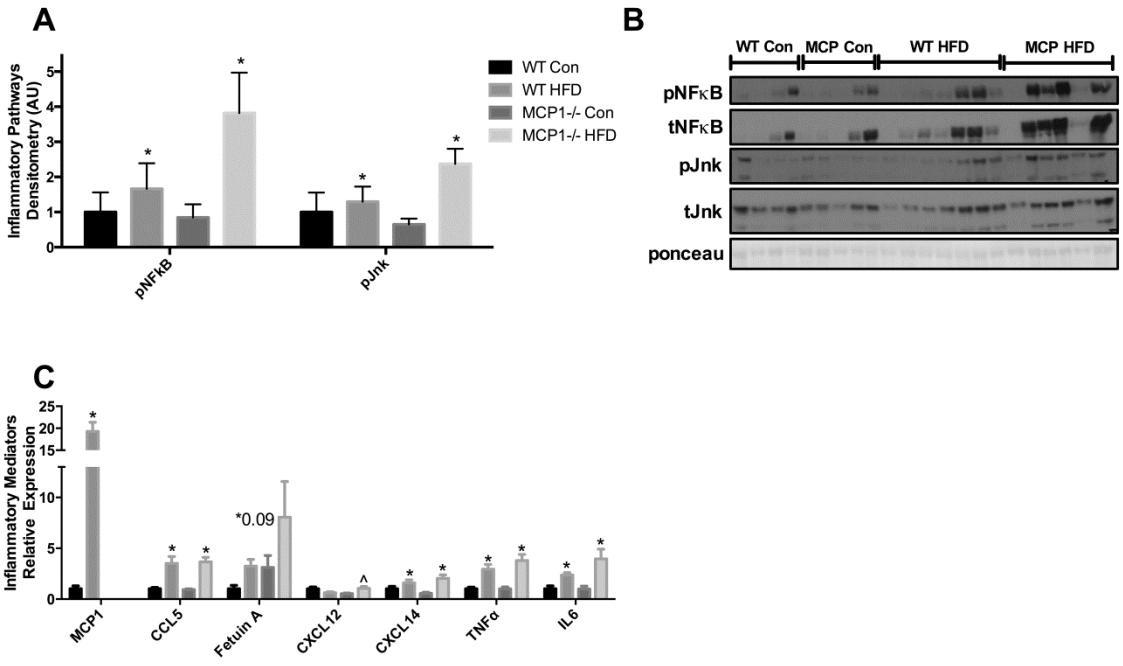


Figure 2.4:

Inflammatory response. A-B. Epididymal fat western blot analysis of inflammatory pathway activation. C. Relative mRNA expression of inflammatory cytokines and chemokines in epididymal fat. *main effect of diet, #main effect of genotype. ^interaction between HFD groups. Data are represented as ± SEM and representative of two individual experiments, n=7 WT Con, n=7 WT HFD, n=7 MCP Con, n=8 MCP HFD.

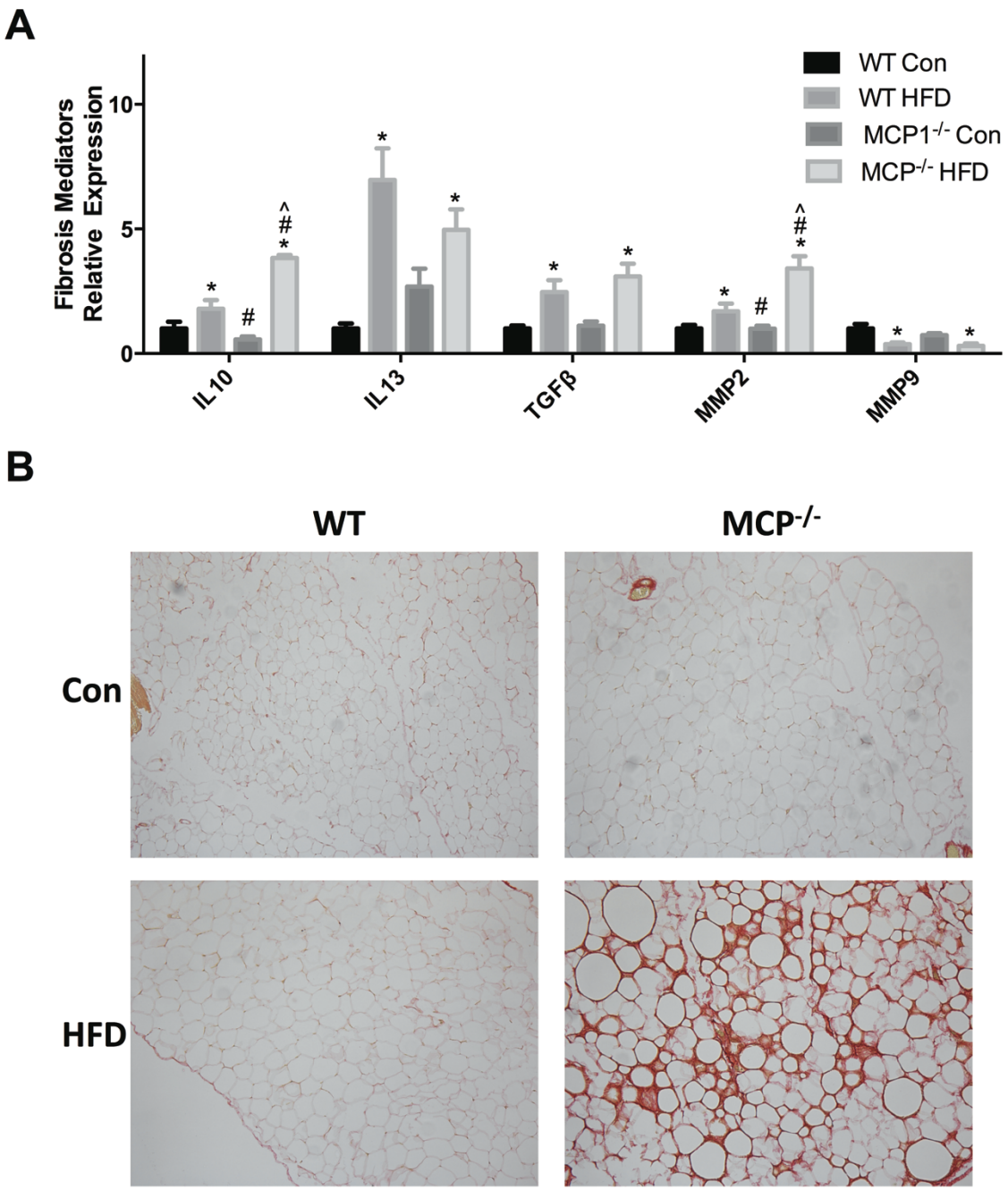


Figure 2.5:

Markers of fibrosis. A. Relative mRNA expression of fibrosis markers in epididymal fat. B. Picro-sirius red staining of epididymal adipose tissue. *main effect of diet, #main effect of genotype. ^interaction between HFD groups. Data are represented as ± SEM and representative of two individual experiments, n=7 WT Con, n=7 WT HFD, n=7 MCP Con, n=8 MCP HFD.

Table 2.1:

Animal characteristics, including liver and fat pad weights, separated by mouse genotype and diet groups. *main effect of diet, #main effect of genotype. ^interaction between HFD groups. Data are represented as ± SEM and representative of two individual experiments, n=7 WT Con, n=7 WT HFD, n=7 MCP Con, n=8 MCP HFD.

| Tissue Weight (mg) | WT Control | MCP1$^{-/-}$ Control | WT HFD | MCP1$^{-/-}$ HFD |
|---|---|---|---|---|
| Epididymal Fat | 594.4±64.5 | 595.1±101.5 | 1516.5±114.5* | 1313.3±117.0* |
| Kidney Fat | 302.3±42.5 | 389.0±78.0 | 978.7±56.8* | 1183.5±89.8*# |
| Mesenteric Fat | 430.9±39.2 | 431.1±56.7 | 1007.0±74.1* | 1137.4±103.1* |
| Total Visceral Fat | 1327.6±141.9 | 1415.3±228.0 | 3379.9±215.6* | 3634.1±233.6* |
| Liver | 1496.8±68.5 | 1667.3±73.6 | 1886.6±67.7* | 2213.0±171.8*# |

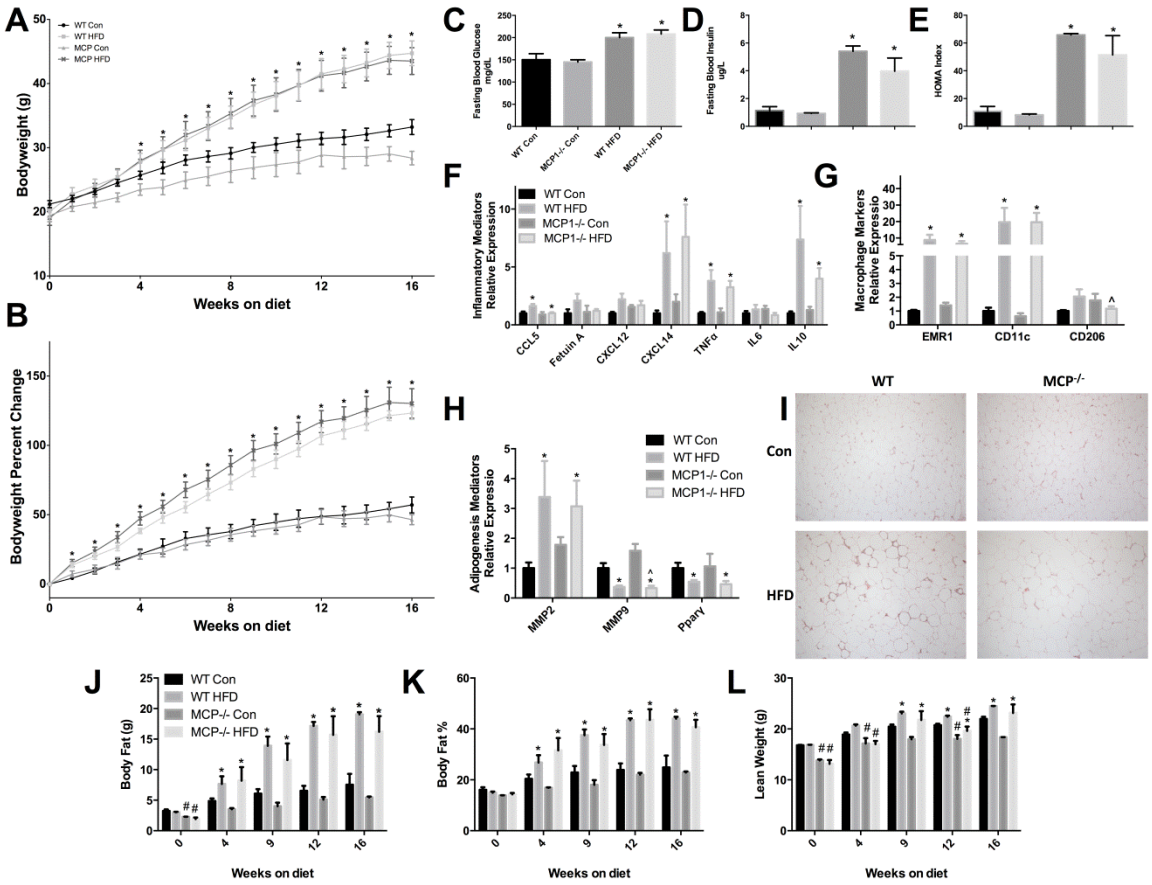


Figure 2.6:

C57BL/6 study results. A. Bodyweight in grams. B. Bodyweight represented as percent change from starting weight. C. Fasting blood glucose concentrations (mg/dL). D. Fasting blood insulin concentrations (ug/L). E. HOMA Index. F. Relative mRNA expression of inflammatory cytokines and chemokines in epididymal fat. G. Relative mRNA expression of macrophage markers in epididymal fat. H. Relative mRNA expression of fibrosis markers in epididymal fat. I. Epididymal fat H&E staining. J. Body composition analysis, Body fat in grams. K. Body fat percentage. L. Lean weight in grams. *main effect of diet, #main effect of genotype. ^interaction between HFD groups. Data are represented as ± SEM, n=6 WT Con, n=5 WT HFD, n=4 MCP Con, n=6 MCP HFD

# CHAPTER 3

# LOSS OF MONOCYTE CHEMOATTRACTANT PROTEIN 1 EXPRESSION DECREASES MAMMARY TUMORIGENESIS AND REDUCES LOCALIZED INFLAMMATION IN THE C3(1)/SV40TAG TRIPLE NEGATIVE BREAST CANCER MODEL[1]

[1] Cranford TL, Velazquez KT, Enos RT, Bader J, Carson MS, Chatzistamou I, Nagarkatti M, Murphy EA. Loss of monocyte chemoattractant protein 1 expression decreases mammary tumorigenesis and reduces localized inflammation in the C3(1)/SV40Tag triple negative breast cancer model *(Submitted to Cancer Biology & Therapy)*

*Abstract*

Monocyte chemoattractant protein 1 (MCP-1) has been implicated as a major modulator in the progression of mammary tumorigenesis, largely due to its ability to recruit macrophages to the tumor microenvironment. Macrophages are key mediators in the connection between inflammation and cancer progression and have been shown to play an important role in tumorigenesis. Thus, MCP-1 may be a potential therapeutic target in inflammatory and difficult-to-treat cancers such as triple negative breast cancer (TNBC). We examined the effect of MCP-1 depletion on mammary tumorigenesis in a model of TNBC. Female C3(1)/SV40Tag and C3(1)/SV40Tag MCP-1 deficient mice were progressed to 12 or 23 weeks of age. Tumor palpations were conducted weekly to establish crude tumor number and volume characteristics. Tumor statistics for number and volume, and gene expression of macrophage markers and inflammatory mediators were measured in the mammary gland and tumor microenvironment at sacrifice. As expected, MCP-1 depletion resulted in decreased tumorigenesis, indicated by reduced primary tumor volume and multiplicity, and a delay in tumor progression represented by histopathological scoring. Deficiency in MCP-1 significantly downregulated expression of macrophage markers in the mammary gland (Mertk and CD64) and the tumor microenvironment (CD64), and also reduced expression of inflammatory cytokines in the mammary gland (TNFα and IL-1β) and the tumor microenvironment (IL-6). These data support the hypothesis that MCP-1 expression contributes to increased tumorigenesis via recruitment of macrophages to the tumor environment, thus resulting in increased inflammatory mediators to assist in mammary tumor progression in a model of TNBC.

*3.1 Introduction*

Breast cancer is the most common cancer and the second leading cause of cancer death among women worldwide (151). In the United States alone, close to 250,000 new cases of invasive breast cancer will be diagnosed and over 40,000 breast cancer deaths will occur in the year 2016 (152). The molecular heterogeneity of breast cancers is now well recognized, with at least five different subtypes identified through molecular profiling (96). Triple negative breast cancer (TNBC) represents a subtype that more frequently affects younger women and is associated with a high mortality rate (153, 154). Triple negative cancers represent between 10-20% of breast cancer cases and are defined as tumors that lack the estrogen receptor (ER), progesterone receptor (PR) and human epidermal growth factor receptor type 2 (Her2/neu) that are known to fuel most breast cancers. TNBC often present as interval cancers and are significantly more aggressive than tumors of other molecular subtypes (153, 155, 156). Patients with triple negative cancers have a significantly shorter survival following the first metastatic event (157), and the majority of deaths occur in the first five years following therapy (158).

The majority of breast cancer clinical subtypes respond well to endocrine and targeted Her2 therapies, but due to the lack of well-defined clinical targets, TNBCs are nonresponsive to these treatment options and consequently, chemotherapy is the standard of care treatment (159). In order to treat TNBC more effectively, new molecular targets need to be identified. MCP-1 represents a promising molecular target for therapeutic intervention. MCP-1 (CCL2) is a member of the C-C chemokine family that bind to G protein coupled receptors to regulate macrophage recruitment during wound healing, infection, and inflammation (23). In mammary tumors, overexpression of MCP-1

correlates with increased recruitment of macrophages and infiltration into the tumor environment that can facilitate tumor progression through macrophage-mediated angiogenesis (105) and through secretion of growth and survival factors (48). Recent studies demonstrate that MCP-1 also signals to breast cancer cells to regulate survival and invasion (111) as well as promote primary tumor growth (112). These reports indicate that MCP-1 regulates multiple mechanisms of breast cancer progression, thus demonstrates MCP-1 value as a potential therapeutic target. However, it's role in TNBC has not yet been fully elucidated.

The purpose of this study was to examine the role of MCP-1 on mammary tumorigenesis in the triple negative C3(1)SV40Tag transgenic mouse model of breast cancer. This was done by crossing the C3(1)SV40Tag mouse, with an MCP-1 knockout mouse to develop an MCP-1 deficient model of mammary tumorigenesis. C3(1)SV40Tag mice lack expression of ER, PR and Her2/neu, and the absence of these has been associated with poor prognosis (160). The overexpression of the early region of SV40 in the mammary epithelium induces mammary tumors in this model is due, at least in part, to Tag inactivation of the tumor suppressors p53 and Rb. The expression of this transgene results in the progressive development of mammary lesions that lead to invasive carcinoma formation (161). C3(1)SV40Tag mice develop mammary epithelial atypia at 8 wks. of age that progresses to mammary intraepithelial neoplasia (MIN) at 12 wks., which is histologically similar to human ductal carcinoma in situ (DCIS). Invasive carcinomas usually develop at approximately 16 wks. of age. We hypothesized that MCP-1 deficiency would reduce primary tumor initiation and tumor growth in a triple negative mouse model of breast cancer and that this would be associated with reduced

macrophage markers and inflammatory mediators in the mammary gland and tumor tissue.

*3.2 Materials & Methods*

Animals

Female FVB/N mice were bred with male heterozygous C3(1)/SV40Tag mice (a gift from Dr. Jeffrey Green, Chief, Transgenic Oncogenesis and Genomics Section, Laboratory of Cancer Biology and Genetics, National Cancer Institute). The MCP1$^{-/-}$ mice on the FVB/N background were developed in our lab. Briefly, FVB/N mice were crossed with the C57BL/6 MCP1$^{-/-}$ strain, and then back-crossed an additional eight times to derive the FVB/N MCP1$^{-/-}$ strain (42). Female MCP1$^{-/-}$ FVB/N mice were then bred with male heterozygous C3(1)/SV40Tag MCP1$^{-/-}$ mice to derive the C3(1)SV40/Tag MCP1$^{-/-}$ strain on the FVB/N background. Female C3(1)/SV40Tag and C3(1)/SV40Tag/MCP$^{-/-}$ offspring were used in these experiments. All experimental mice were bred and cared for in the animal research facility at the University of South Carolina. They were housed, 2-5/cage, maintained on a 12:12-h light-dark cycle in a low stress environment (22°C, 50% humidity, low noise) and given food and water *ad libitum*. Principles of laboratory animal care were followed, and the Institutional Animal Care and Usage Committee of the University of South Carolina approved all experiments.

Genotyping protocol

Female C3(1)/SV40Tag and C3(1)/SV40Tag/MCP$^{-/-}$ mice were used in all experiments and were genotyped by tail snip at 3 weeks of age for the C3(1) 5' flanking sequence and MCP-1 gene ablation status using the primer sequences as follows:

C3(1) forward - CAG TGG TTC CCA GAG TCT CA

Tag reverse - CAG AAG CCT CCA AAG TCA GG

MCP-1 Common - TCA TTG GGA TCA TCT TGC TG

MCP-1 Wild-type - TGA CAG TCC CCA GAG TCA CA

MCP-1 Mutant - GCC AGA GGC CAC TTG TGT AG

A snip of mouse tail is added to 150ul of DirectPCR tail buffer (Viagen Biotech Inc, Los Angeles, CA) and 2ul of Proteinase K (Viagen Biotech Inc, Los Angeles, CA) and digested at 55°C overnight. The next day samples were incubated at 95°C for an hour then added to a PCR cocktail for amplification. The PCR cocktail contains DNA template, upstream and downstream primers, dd$H_20$, and GoTaq Green Master Mix (Promega Corp, Madison, WI). Samples were run on 2% agarose gel and compared to control samples to determine genotype (556 base pair molecular weight for C3(1)/SV40Tag positive samples).

Body weights and tumor palpations

Body weight was monitored weekly. C3(1)/SV40Tag mice typically develop palpable mammary tumors between 12 and 16 weeks of age (162). Tumors were palpable beginning at 12 weeks of age and were measured weekly by the same investigator. Upon palpation of a tumor, calipers were used to measure the longest and shortest diameter of the tumor. The number of tumors within each mouse was recorded and the tumor volume

was estimated for each tumor using the formula: 0.52 X (largest diameter) X (smallest diameter)$^2$ as previously described (163).

Diets

The AIN-76A diet was administered to all experimental groups beginning at 4 weeks of age (Bioserv, Frenchtown, NJ) (51). AIN-76A is a purified, balanced diet that is phytoestrogen free. Dietary phytoestrogens have been shown to influence anxiety-related behaviors, fat deposition, blood insulin, leptin and thyroid levels as well as lipogenesis and lipolysis in adipocytes (164).

Tissue collection

At 23 weeks of age mice were sacrificed for tissue collection. An additional group of mice were sacrificed at an earlier time point (12 weeks of age) for histopathological analysis and comparison. Palpable tumors were dissected from mammary glands and measured grossly to determine tumor volume. A portion of the remaining thoracic mammary gland tissue was then removed from both the right and left side. This tissue was either snap frozen in liquid nitrogen for gene expression analysis or fixed in 4% formaldehyde for immunohistochemical analysis.

Histology

At sacrifice, a portion of mammary gland adipose tissue was excised from each mouse, fixed overnight in 4% formaldehyde, dehydrated with 70% alcohol, and embedded in wax. Paraffin sections were stained with hematoxylin and eosin (H&E). The mammary gland from mice aged 12 and 23 weeks was subsequently evaluated blindly by a pathologist and characterized according to histological alterations observed and the grade of dysplastic changes existed as: no hyperplasia or dysplasia, atypical

ductal hyperplasia (ADH)/mammary intraepithelial neoplasia (MIN) low grade, ductal carcinoma in situ (DCIS)/MIN high grade, or invasive adenocarcinoma (162).

Real-time quantitative PCR

Mammary adipose tissue total RNA was extracted using Qiagen AllPrep DNA/RNA/Protein minikit (Qiagen, Germantown, MD). Briefly, DNA was bound to DNAEasy columns supplied by the kit and isolation was performed according to manufacturer instructions. 100% ethanol was added to the flow through from the DNA bound columns which contained the RNA. The RNA-containing flow through was then bound to the RNAEasy columns supplied by the kit and centrifuged for 15s and 8000 x g. A series of washes were performed using proprietary buffers included with the kit and the RNA was eluted using RNA-free water. Primary tumor tissue total RNA was extracted using TRIzol reagent (Invitrogen, Carlsbad, CA) and chloroform/isopropyl alcohol extraction as previously described (165). Quantification of mammary adipose tissue mRNA gene expression was performed for macrophage markers (CD64 (Fcgr1), Mertk), cytokines (interleukin (IL)-6 (IL-6), tumor necrosis factor α (TNFα), IL-1β, IL-12, IL-10), and the chemokine (MCP-1). Quantification of primary tumor mRNA gene expression was performed for macrophage markers (CD64 and Mertk) and cytokines (IL-6, TNFα, and IL1β) (Applied Biosystems, Foster City, CA) as previously described (138). RNA quality and concentration was analyzed using a NanoPhotometer Pearl (Implen, Westlake Village, CA). Murine 18s rRNA was used as the housekeeping gene to normalize all of the data obtained. Quantitative reverse transcriptase polymerase chain reaction analysis was carried out as per the manufacturer's instructions and all gene expression primers were TaqMan Gene Expression Assays (Applied Biosystems, Foster

City, CA). Quantification of mRNA expression of all target genes was calculated using the $2\Delta\Delta C_T$ method.

Statistical analysis

All data were analyzed using commercial software (GraphPad Software, Prism 7, La Jolla, CA, USA). A two tailed t-test was used to compare differences across groups. Statistical significance was set with an $\alpha$ value of $P \leq 0.05$. Data are represented as mean ± SEM.

*3.3 Results*

MCP-1 deficiency decreases tumor volume and tumor number in mammary primary tumor palpations

Body weight measurements were taken weekly throughout the experimental period to confirm normal growth patterns following deletion of MCP-1. MCP-1 ablation did not significantly alter total body weight for the C3(1)/SV40Tag/MCP-$1^{-/-}$ mice when compared to the MCP-1 sufficient mice at any point during the experiment (Figure 3.1A). Treatment groups reported final body weight measurements of 24.25g±0.65 and 22.94g±0.90 for C3(1)/SV40Tag and C3(1)/SV40Tag/MCP-$1^{-/-}$ groups, respectively. Tumor palpations began at 12 weeks of age and continued until 22 weeks of age, which allowed us to crudely measure tumor burden between groups without anesthetizing the animals. C3(1)/SV40Tag mice experienced significant increases in primary tumor number beginning at 16 weeks of age (1.33±0.35 compared to 0.25±0.18 for MCP-1 deficient mice) and continued until the final week (age 22 weeks) of palpation

measurements (4.20±0.33 compared to 1.67±0.31 for C3(1)/SV40Tag/MCP-1$^{-/-}$ mice) (Figure 3.1B) ($P<0.05$). Both experimental groups had similar trends in primary tumor volume growth throughout the experiment until week 22 when the C3(1)/SV40Tag mice had a significantly large increase in tumor volume growth (1033.05±324.35mm$^3$) compared to the MCP-1 deficient mice (246.78±119.34mm$^3$) (Figure 3.1C) ($P<0.05$).

Loss of MCP-1 results in decreased primary tumor initiation and tumor volume

Measurements taken at sacrifice for total primary tumor volume and total primary tumor number for animals in each group indicated significant differences in tumorigenesis with MCP-1 manipulation in this model of TNBC. MCP-1 expression resulted in significantly increased primary mammary tumor multiplicity and growth compared to the MCP-1 deficient group; mean tumor number/mouse (Figure 3.2A) and mean tumor volume/mouse (Figure 3.2B) determined at necropsy were 15.86±1.07 and 3126.62±771.83 mm$^3$ for C3(1)/SV40Tag, and 6.67±1.46 and 935.78±232.11 mm$^3$ for C3(1)/SV40Tag/MCP-1$^{-/-}$ mice, respectively ($P<0.05$).

Deletion of MCP-1 expression delays tumor progression in the early stages of tumorigenesis

There was no difference in the percentage of samples classified in each pathological stage between the groups at 23 weeks of age (Figure 3.3A). The early stage of tumorigenesis in this model is classified as atypical ductal hyperplasia (ADH, low grade MIN lesion), which is characterized as having more than one layer of disorganized and atypical epithelial cells with frequent mitotic figures, lining the mammary ducts. In the current investigation, 15.4% of C3(1)/SV40Tag and 10.0% of C3(1)/SV40Tag/MCP-1$^{-/-}$ mice classified into this early tumorigenic stage. The next progressive level is ductal

carcinoma in situ (DCIS, high grade MIN lesion), classified as the filling and expansion of ducts with highly dysplastic epithelial cells confined still in the ducts without breaching the underlying basal lamina. We report that 30.8% and 30.0% of samples for C3(1)/SV40Tag and C3(1)/SV40Tag/MCP-1$^{-/-}$ mammary glands scored into this stage, respectively. The final stage is invasive adenocarcinoma which is described as poorly differentiated adenocarcinoma characterized by sheets of neoplastic cells occasionally forming glandular structures separated by fine fibrovascular stroma (166). The majority of mice in the current study were classified into this advanced stage; 53.8% C3(1)/SV40Tag and 60% of C3(1)/SV40Tag/MCP-1$^{-/-}$ mice (Figure 3.3A). These findings imply that there were no differences in the pathology between the experimental groups at this stage of tumorigenesis. However, this may not be entirely surprising given the advanced stage of tumorigenesis at which these analyses were performed. Therefore, we performed an additional experiment in which the histopathology was examined at a much earlier stage of tumorigenesis (i.e. 12 weeks of age) (Figure 3.3A). By 12 weeks of age, this cancer model is characterized by progression into MIN/high grade (162). Consistent with the tumor burden data, histopathology in the mammary gland of mice sacrificed at 12 weeks of age clearly showed a delay in tumor progression for MCP-1 deficient mice compared to C3(1)/SV40Tag mice. We report that 50% of the C3(1)/SV40Tag animals progressed into this high grade lesions (MIN, high grade), while 50% of samples were of low grade lesions (MIN, low grade); whereas, 100% of MCP-1 deficient mice remain classified into the early atypical ductal hyperplasia (ADH). Figure 3.3B-D are representative images of tumorigenesis of each histopathological stage for this TNBC mouse model.

MCP-1 deficiency results in a decline of macrophage markers and localized inflammatory mediators in the mammary gland and tumor microenvironment

At 23 weeks of age, the mRNA expression of the macrophage marker, Mertk, was significantly downregulated in the mammary gland of MCP-1 deficient mice ($P<0.05$), while macrophage marker CD64 had a decreasing downtrend with $P=0.06$ (Figure 3.4A). Pro-inflammatory cytokine IL-1β was significantly decreased ($P<0.05$), whereas, pro-inflammatory cytokines IL-6 and TNFα indicated a downtrend in mRNA expression in the mammary gland with $p=0.09$ and $p=0.06$, respectively. Cytokines IL-12 and IL-10 had no change in mRNA expression in the mammary gland and, as expected, MCP-1 expression was not detected in the mammary gland of C3(1)/SV40Tag/MCP-$1^{-/-}$ mice, thus confirming their knockout genotype status (Figure 3.4B).

Deletion of MCP-1 expression resulted in a significant decrease in mRNA expression of macrophage marker CD64 in the tumor environment ($P<0.05$) but there was no significant change in Mertk expression (Figure 3.4C). MCP-1 ablation also significantly downregulated mRNA expression of the pro-inflammatory cytokine IL-6 in the tumor environment ($P<0.05$); however, there was no change in TNFα and IL-1β expression in the tumor environment (Figure 3.4D).

*3.4 Discussion*

Studies indicate that MCP-1 regulates multiple mechanisms of breast cancer progression (48). Experimental evidence has shown MCP-1 to be the major chemokine for macrophage recruitment into the tumor microenvironment (167), a process that is known to drive tumorigenic events. However, the importance of this chemokine in the

progression of tumorigenesis in a triple negative model of breast cancer has not been well established. Therefore, using a gene deletion approach in the C3(1)SV40Tag mouse, we developed a C3(1)SV40Tag/MCP-1$^{-/-}$ mouse to examine the effects of MCP-1 deficiency on TNBC that is closely associated with poor prognosis in human breast cancer. Results show that deficiency of MCP-1 reduces mammary tumorigenesis with a significant decrease in primary tumor volume and tumor number. Consistent with the primary tumor data, histopathology in the mammary gland of mice sacrificed at an early time point, but well established stage for this breast cancer model, showed a delay in tumor progression for MCP-1 deficient mice. MCP-1 deficient mice showed a reduction in mRNA expression of macrophage markers (CD64 and Mertk) and inflammatory cytokines in the mammary gland that are known to play a role in breast cancer progression (64, 110). Additionally, tumor tissue gene expression of the macrophage markers CD64 and inflammatory cytokine IL-6 were also significantly reduced in the MCP-1 deficient mice. These data support a beneficial effect of MCP-1 deficiency on mammary tumorigenesis in the C3(1)/SV40Tag mouse model of TNBC that is associated with a reduction in macrophage markers and inflammatory mediators in the mammary gland and tumor environment.

Both rodent and clinical studies have associated MCP-1 expression level with tumorigenesis (48, 168, 169). Our results are consistent with previous studies that have linked MCP-1 gene knockdown or ablation with a reduction in primary tumorigenesis in various cancer models. In a study previously conducted by our laboratory, MCP-1 deficiency resulted in a reduction of overall intestinal polyp number in a mouse model of intestinal tumorigenesis (170). Similarly, Fridlander *et al*., demonstrated a beneficial

effect of MCP-1 neutralization in a murine model of non-small cell lung cancer (171). However, there have been relatively few mechanistic studies to link MCP-1 expression to breast cancer progression, and in particular TNBC. MCP-1 is expressed at relatively low levels in normal mammary epithelial tissue and circulating plasma, but increases dramatically with breast cancer progression (48, 117, 172, 173). Recently, MCP-1 has been shown to signal to breast cancer cells to regulate survival and invasion (111), promote primary tumor growth (112), and mediate breast cancer metastasis (174). Interestingly, TNBC educated macrophages secrete higher amounts of MCP-1 than macrophages co-cultured with estrogen receptor positive breast cancer (175). Most likely, cancer cell/macrophage crosstalk in TNBC initiates a vicious circle where both cell types reinforce each other (176, 177). MCP-1 also correlates with high tumor grade, increased metastasis and is associated with low levels of cell differentiation and poor prognosis in breast cancer (178). In a study previously conducted by our laboratory, we utilized a pharmacological approach and examined the effects of an MCP-1 inhibitor on mammary tumorigenesis in this same C3(1)SV40Tag mouse model. The chemical MCP-1 inhibitor led to a significant reduction in tumor multiplicity but did not delay the initial palpable tumor nor slow the tumor growth as tumor volume and latency were similar between treatment groups (47). A potential limitation of that study was the long term treatment protocol used as the inhibitor was given in the food for a period of 16 weeks. Thus, it is possible that the animals developed a tolerance to the inhibitor treatment as a decrease in circulating levels of MCP-1 in plasma was not observed. This suggests that the overall effectiveness of the treatment dose, timing and administration method may not have been optimal in this animal model. Given the promising results of MCP-1

inhibition, but also considering the limitations of that study, we developed the MCP-1 global knockout C3(1)SV40Tag mouse to more conclusively examine the role of MCP-1 on TNBC. In the present investigation, we show for the first time that genetic knockdown of MCP-1 expression can lead to a significant reduction in mammary tumor volume and multiplicity in the C3(1)SV40Tag transgenic mouse model of TNBC.

Macrophages play a key role in tumorigenesis; they are a major player in the inflammatory response that contributes to cellular proliferation, transformation, promotion, invasion, angiogenesis, apoptosis and metastasis (106, 179). Given that MCP-1 has been implicated as the most important chemokine for macrophage recruitment into the tumor microenvironment, we next examined the effect of MCP-1 deficiency on select macrophage markers in the mammary tissue and tumor microenvironment. In the past several years, considerable progress has been made in distinguishing macrophages from dendritic cells, two immune cells of similar origin reflected by overlapping functions and molecular profiles. More recently, two mRNA transcripts that are unique to macrophages and not dendritic cells have been identified; Mer tyrosine kinase receptor (Mertk), which is involved in the phagocytosis of apoptotic cells, and Fcgr1, which encodes the immunoglobulin receptor CD64 on macrophages (180). Studies have implicated Mertk to not only be highly elevated in human breast carcinoma samples, but also mediate efferocytosis in macrophages and advance tumor progression through the inhibition of immune checkpoints (181). In this experiment, MCP-1 depletion resulted in a reduction in both Mertk and CD64 mRNA expression in the mammary gland, and also CD64 mRNA expression in the tumor tissue. These results are consistent with a very recent study in which Fang *et al*., demonstrated a reduction in

the recruitment of macrophages to the tumor microenvironment with targeted MCP-1 gene silencing in a model of TNBC cancer (112). Similarly, previous work by our group has shown equivalent results using pharmacological inhibition of MCP-1 in TNBC (47). These findings should be substantiated through the use of cell sorting to solidly establish the role of MCP-1 depletion on macrophage infiltration and specific macrophage phenotypes that may be associated with TNBC.

Studies have established that the mutual interaction of macrophages with cancer cells enhances survival, invasion, promotes primary tumor growth and increases the production of inflammatory cytokines to transform the tumor microenvironment so that it favors tumorigenesis (111, 112). The inflammatory cytokines TNFα, IL-1β, and IL-6 have been associated with poor prognosis and increasing risks of metastasis in breast cancer in addition to being related to tumor macrophage expression of MCP-1 (48, 110). We investigated the expression of these inflammatory cytokines in the surrounding dysplastic mammary tissue and in the tumor environment. Our findings indicate that the absence of MCP-1 expression significantly corresponds with decreases in mRNA expression of TNFα, IL-1β, and IL-6 in the mammary gland and decreases in IL-6 expression in the tumor. These data are supported in a study by Ueno *et al*, that demonstrated MCP-1 expression levels are associated with IL-6 expression levels in human breast cancer tissues (48). There is consistent data showing increased levels of IL-6 in breast cancer patients when compared to healthy controls and increased levels of IL-6 have also been correlated with clinical tumor stage, lymph node infiltration and recurrent disease (182). IL-6 levels have also been associated with poor prognosis for time-to-progression and death in advanced stage patients (183).

In summary, we report for the first time that ablation of MCP-1 expression through genetic deletion results in decreased mammary tumorigenesis and downregulated localized inflammation in the C3(1)/SV40Tag model of TNBC. Although, MCP-1 expression has been connected with regulating multiple mechanisms of breast cancer progression, its involvement in tumorigenesis in a TNBC model has not been fully established. MCP-1 provides a direct link between inflammation and macrophage recruitment and not surprisingly, therefore has an emergent role in the etiopathogenesis of breast cancer. Given the profound clinical implications, more research is needed to fully elucidate the role of this chemokine in breast cancer progression so that targeted therapies can be developed.

*3.5 Figures & Legends*

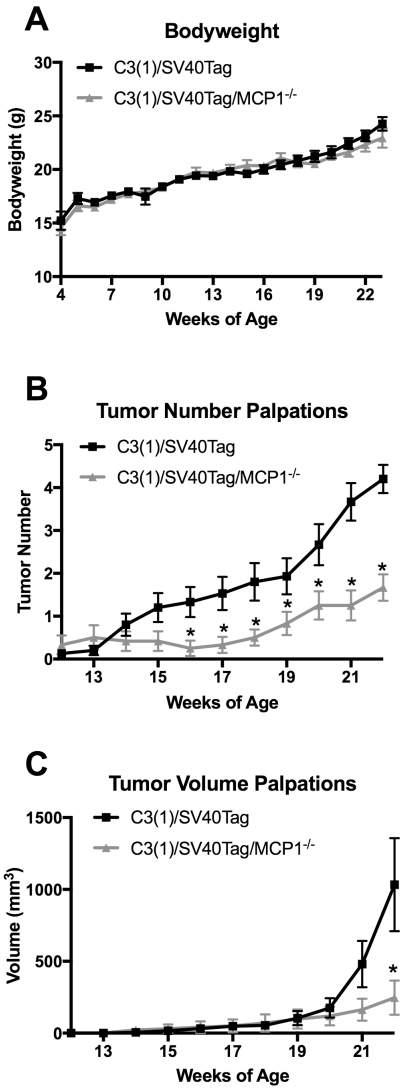


Figure 3.1:

Body weight characteristics and tumor palpations. A. Body weight in grams. B. Tumor number palpations. C. Tumor volume palpations. *P<0.05. Data are represented as ± SEM, C3(1)/SV40Tag n=15, C3(1)/SV40Tag/MCP-1$^{-/-}$ n=12.

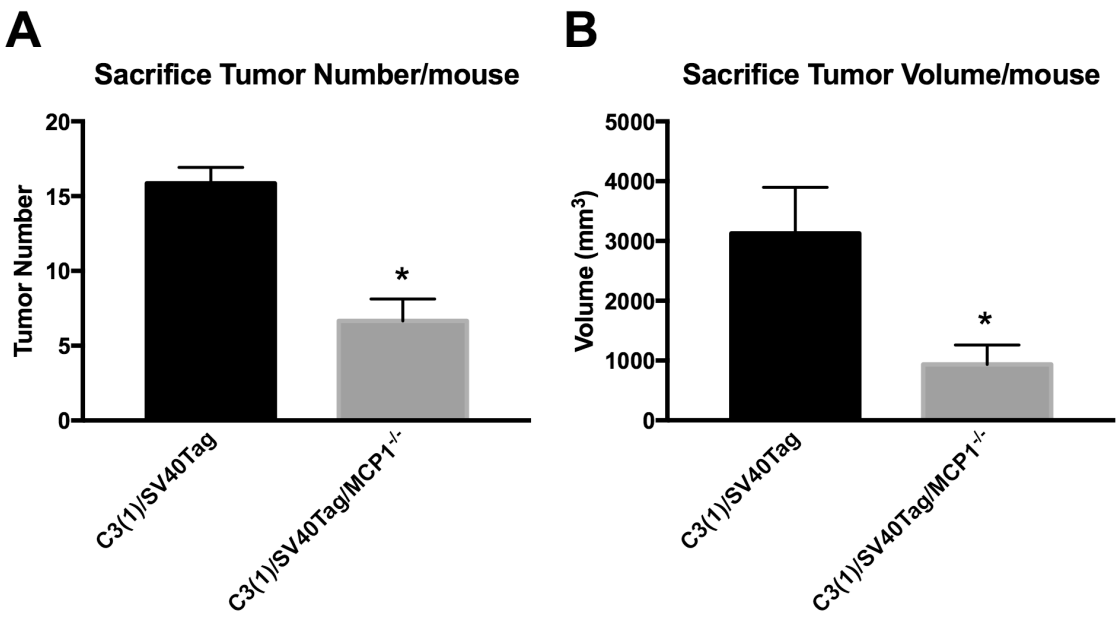


Figure 3.2:

Tumor statistics at necropsy. A. Total tumor number per mouse taken at necropsy. B. Total tumor volume per mouse taken at necropsy. *P<0.05. Data are represented as ± SEM, C3(1)/SV40Tag n=15, C3(1)/SV40Tag/MCP-1$^{-/-}$ n=12.

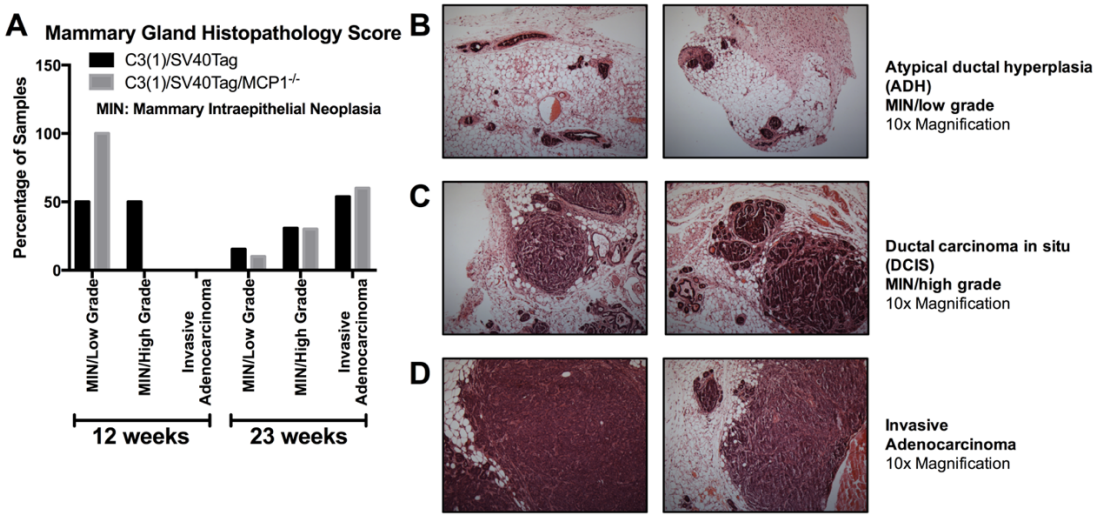


Figure 3.3:

Mammary gland histopathology for each treatment group. A. Graph of mammary gland pathology score for mice at 12 weeks and 23 weeks of age for both groups. B. Representative images of atypical ductal hyperplasia (ADH, low grade MIN lesion) characterized by several layers of disarranged atypical epithelial cells with frequent mitotic figures. C. Representative images of ductal carcinoma in situ (DCIS, high grade MIN lesion) characterized by filling and expansion of ducts with dysplastic epithelial cells without breach of the basement membrane or invasion of the surrounding adipose tissue. D. Representative images of invasive adenocarcinoma characterized by pleomorphic neoplastic cells arranged in sheets or in tubules separated by fine fibrovascular stroma. Figures B-D shown at 10x magnification. Data are represented as percentage of total samples for each time point/group, 12-week time point: C3(1)/SV40Tag n=6, C3(1)/SV40Tag/MCP-1$^{-/-}$ n=5, 23-week time point: C3(1)/SV40Tag n=15, C3(1)/SV40Tag/MCP-1$^{-/-}$ n=12.

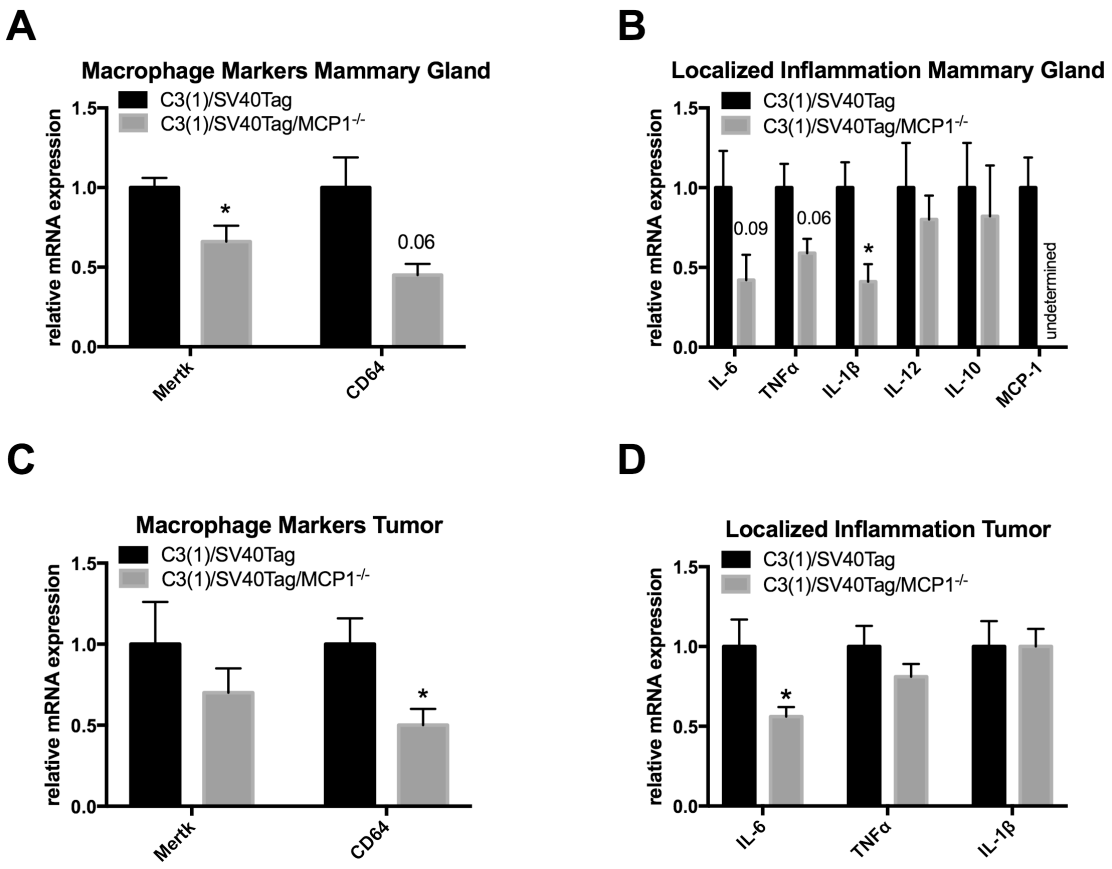


Figure 3.4:

Macrophage markers and localized inflammation in the mammary gland and tumor. A. Relative gene expression of macrophage markers in the mammary gland. B. Relative gene expression of inflammatory mediators in the mammary gland. C3(1)/SV40Tag n=10, C3(1)/SV40Tag/MCP-1$^{-/-}$ n=7. C. Relative gene expression of macrophage markers in the tumor. D. Relative gene expression of inflammatory mediators in the tumor. *P≤0.05. Data are represented as ± SEM, C3(1)/SV40Tag n=13, C3(1)/SV40Tag/MCP-1$^{-/-}$ n=10.

# CHAPTER 4

# EFFECTS OF HIGH FAT DIET-INDUCED OBESITY ON MAMMARY TUMORIGENESIS IN THE PYMT/MMTV MURINE MODEL[1]

[1] Cranford TL, Velazquez KT, Enos RT, Bader J, Carson MS, Fan D, Bellone RR, Chatzistamou I, Nagarkatti M, Murphy EA. Effects of high fat diet-induced obesity on mammary tumorigenesis in the PyMT/MMTV murine model *(Manuscript in Preparation)*

*Abstract*

Clinical studies provide strong evidence that obesity and associated adipose tissue inflammation are risk factors breast cancer; however, mechanistic knowledge of the interaction of obesity, breast cancer and menopausal status has proven to be not only lacking, but contradictory. Obesity-induced inflammation and elevated biosynthesis of estrogens, through aromatase-mediated metabolism of precursors, have been linked with hormone receptor positive (HP) postmenopausal breast cancer but not previously associated with premenopausal breast cancer risk. Thus, further delineation of the interaction of obesity, inflammation, and aromatase is required for the development of therapeutic treatment options. The purpose of this study was to examine the effect of high fat diet (HFD)-induced inflammation on tumorigenesis in a model of pre and postmenopausal HP breast cancer. Female PyMT/MMTV ovary intact and ovariectomized mice were fed low and HFD diets to examine the role of obesity-induced inflammation and hormone production in the development of HP breast cancer. Tumor statistics for number, volume, weight, histopathology scoring and gene expression of macrophage and inflammatory mediators were measured in the adipose tissue and mammary gland at sacrifice. HFD feedings of ovary intact mice resulted in increased adiposity and tumorigenesis, indicated by increased primary tumor volume, multiplicity, tumor burden, and increased tumor progression represented by histopathological scoring. HFD-induced obesity significantly upregulated aromatase and macrophage marker expression in the adipose tissue (F4/80 and CD11c) and mammary gland (Mertk) in a premenopausal model of breast cancer. Conversely, HFD feedings had no significant effect on tumorigenesis in a postmenopausal model of breast cancer despite large increases in adiposity in ovariectomized mice. This data suggests that obesity-induced

increases in inflammation and hormone production, via aromatase expression, is associated with increases in tumorigenesis in a model of premenopausal HP breast cancer in the PyMT/MMTV strain.

*4.1 Introduction*

The etiopathogenesis of breast cancer is elaborate and involves the interaction of genetic and environmental factors. Epidemiological studies provide strong evidence to suggest that obesity is a risk factor for breast cancer. However, inconsistencies in the literature imply that the complexity of the relationship between breast cancer and obesity remains inadequately understood. In the case of younger women, the link between body mass and breast cancer risk is controversial. Some clinical studies report a null or inverse association between obesity and breast cancer risk (69-72), a few epidemiological studies suggest reduced overall risk of premenopausal breast cancer associated with obesity (184), while other investigators report weight gain and central obesity increase the risk of premenopausal breast cancer (73-77). In postmenopausal women the relationship is clearer; the majority of evidence supports a direct link between obesity and the risk for certain clinical subtypes of breast cancer (78-81). For instance, cohort and case control studies indicate that obesity is an independent risk factor for postmenopausal estrogen receptor positive (ER+) and progesterone receptor positive (PR+) breast cancer (80, 81, 84, 86, 89, 185) and experimental studies in mice substantiate these claims (81, 186-189). Women with the greatest increase in weight have higher risk at older ages and this association appears to be stronger for HP tumors (190). Given that two out of three women in the United States are overweight or obese, an understanding of the mechanisms

that link obesity to breast cancer, and the connection with menopausal status, is of critical public health importance.

A number of mechanisms are likely to link obesity to breast cancer. However, inflammation is arguably at the forefront. Chronic inflammation is recognized as an important mediator in the clinical and biochemical complications associated with obesity and also breast tumor biology and causation. Inflammation in adipose tissue, with infiltration by macrophages, is a well-established characteristic of obesity and its presence in the breast creates local conditions that favor breast epithelial cell transformation, cancer cell proliferation and invasion, as well as, tumor-related neovascularization, that contribute to poor prognosis. Further, obesity-mediated inflammation has been reported to drive estrogen synthesis, which increases the risk of HP breast cancer; previous studies have linked the upregulation of adipose tissue pro-inflammatory cytokines with the expression of the estrogen synthase cytochrome P450 (aromatase) in murine (97) in both pre and postmenopausal human breast cancer (68, 98).

The purpose of this study was to examine mammary tumorigenesis in response to HFD feedings in the PyMT transgenic murine model of tumorigenesis. The PyMT/MMTV is an experimental model that presents morphological similarities with human breast carcinoma. In this model, the expression of the oncoprotein, polyoma virus middle T antigen, is under the control of the mouse mammary tumor virus promoter and is therefore restricted to the mammary epithelium (191). In addition to the tumor progression similarities, the expression of biomarkers in PyMT-induced tumors, to include the loss of ER+ and PR+ receptors and overexpression of ErbB2/Neu/HER2 as the cancer progresses to malignancy, is also consistent with those associated with poor

outcome in human breast cancer. While the majority of studies investigating the relationship between HFD-induced obesity and mammary tumorigenesis have been performed in the FVB/N background, a strain traditionally shown to be HFD-induced obesity resistant, we utilized the C57Bl/6 background, a strain that is more susceptible to HFD-induced obesity. Further, by utilizing both intact and ovariectomized mice, we were able to evaluate the effects of HFD feedings in a model of pre and postmenopausal breast cancer. Given that inflammation is a likely link between obesity and breast cancer, we further examined changes in inflammatory-related parameters in association with the tumorigenic outcomes.

*4.2 Materials & Methods*

Animals

Male PyMT/MMTV mice on a C57Bl/6 background were randomly bred with female wild-type (WT) mice to obtain female mice heterozygous for the PyMT transgene. Two independent experiments were conducted to examine mammary tumorigenesis as it pertains to menopausal status. The first experiment (Exp1) utilized PyMT ovary intact females and female WT littermates were included as a non-disease control. Mice in Exp1 were sacrificed at 20 weeks of age (16 weeks of diet treatment). The second experiment (Exp2) only included PyMT ovariectomized females. At 5 weeks of age, mice underwent ovariectomy surgery and were allowed one week to recover prior to the start of diet treatments. Mice in Exp2 were sacrificed at 24 weeks of age (18 weeks of diet treatment). All experimental mice were bred and cared for in the animal research facility at the University of South Carolina. They were housed, 3-5/cage,

maintained on a 12:12-h light-dark cycle in a low stress environment (22°C, 50% humidity, low noise) and given food and water *ad libitum*. Principles of laboratory animal care were followed, and the Institutional Animal Care and Usage Committee of the University of South Carolina approved all experiments.

Ovariectomy surgery

Mice are briefly anesthetized with isoflurane. The dorsal mid-lumbar area was shaved and swabbed with iodine and alcohol. A 2cm dorsal midline skin incision was made halfway between the caudal edge of the ribcage and the base of the tail. The fascia was cleared away using blunt dissection. A single incision of less than 1cm long was made into the muscle wall on both the right and left sides approximately 1cm lateral to the spine. The ovary and the uterine horns located in the fat pad under the dorsal muscle were extracted through the incisions with forceps. Both uterine horns were tied beneath the ovary with a suture (non-absorbable suture 5-0, cat # S-G518R13) and ovaries were removed with single cuts. The uterine horns were placed back into the peritoneal cavity. Muscle incisions were closed with 5-0 absorbable suture (Cat # S-G518R13-U). Wound clips were used to close skin incision. Animals were examined for incision repair or infection for at least 72 hours post-surgery. Wound clips were removed at 7-day post-surgery.

Genotyping protocol

Female mice were used in all experiments and were genotyped for the PyMT transgene using the primer sequences as follows:

PYVT-1 GGAAGCAAGTACTTCACAAGGG,

PYVT-2 GGAAAGTCACTAGGAGCAGGG.

A snip of mouse tail is added to 150ul of DirectPCR tail buffer (Viagen Biotech Inc, Los Angeles, CA) and 2ul of Proteinase K (Viagen Biotech Inc, Los Angeles, CA) and digested at 55°C overnight. The next day samples were incubated at 95°C for an hour then added to a PCR cocktail for amplification. The PCR cocktail contains DNA template, upstream and downstream primers, $ddH_20$, and GoTaq Green Master Mix (Promega Corp, Madison, WI). Samples were run on 2% agarose gel and compared to control samples to determine genotype (520 base pair molecular weight for PyMT/MMTV positive samples).

Diets

For Exp1, PyMT mice and WT non-disease control mice were randomly assigned to either a low fat diet (LFD) or a HFD treatment group beginning at 4 weeks of age. The AIN-76A diet (11.5% kcal as fat) was used for the LFD (Bioserv, Frenchtown, NJ) (51, 133). AIN-76A is a purified, balanced diet that is phytoestrogen free. Dietary phytoestrogens have been shown to influence anxiety-related behaviors, fat deposition, blood insulin, leptin and thyroid levels as well as lipogenesis and lipolysis in adipocytes (164). The D12492 diet (60% kcal as fat) was used for the HFD (Research Diets, New Brunswick, NJ). Mice were fed their respective diets for 16 weeks.

In Exp2, PyMT mice at 6 weeks of age were randomly assigned to the same LFD and HFD-treatment groups used in experiment 1. Mice were fed their respective diets for 18 weeks.

Body weights, food intake, and body composition

Body weight and food intake were monitored weekly for both experiments. Body composition for WT mice was assessed at the conclusion of the study (20 weeks of age)

in Exp1. PyMT groups were not analyzed for body composition as the tumors can alter lean mass calculations. Briefly, mice were placed under anesthesia (isoflurane inhalation) and were assessed for lean mass, fat mass, and body fat percentage via dual-energy x-ray absorptiometry (DEXA) (Lunar PIXImus, Madison, WI) (51).

Tumor palpations

Tumors were palpable beginning at 14 weeks of age (10 weeks of diet treatment) and 14 weeks of age (8 weeks of diet treatment) for each of Exp1 and Exp2, respectively, by the same investigator. PyMT/MMTV mice typically develop palpable mammary tumors between 12 and 16 weeks of age (191) . Upon palpation of a tumor, calipers were used to measure the longest and shortest diameter of the tumor. The number of tumors within each mouse was recorded and the tumor volume was estimated for each tumor using the formula: 0.52 X (largest diameter) X (smallest diameter)$^2$ as previously described (163).

Tissue collection

Following 16 weeks (Exp1) and 18 weeks (Exp2) of dietary treatment, mice were sacrificed for tissue collection. Visible tumors were dissected from mammary glands and measured to determine tumor weight and tumor volume. A portion of remaining thoracic mammary gland tissue was then removed from both the right and left side. Visceral fat pads were removed. These tissues were either snap frozen in liquid nitrogen for gene expression analysis or fixed in 4% formaldehyde for immunohistochemical analysis.

Histology

A portion of the thoracic mammary gland from both Exp1 and Exp2 was excised from each mouse, fixed overnight in 4% formaldehyde, dehydrated with alcohol, and

embedded in wax. Paraffin sections were stained with hematoxylin and eosin (H&E). The mammary gland was subsequently evaluated blindly by a pathologist and characterized according to the grade of dysplasia: no hyperplasia, adenoma/mammary intraepithelial neoplasia (MIN), and early and late invasive carcinoma for both experiments (191).

PCR cleanup for sequencing of PyMT transgene

PyMT transgene was sequenced to design qPCR primers for verification that diet did not affect transgene expression. One gDNA sample and a cDNA sample from each treatment groups (PyMT Con 4 and PyMT HFD 2) were used for sequencing experiments of the PyMT transgene. gDNA and cDNA were both included to confirm that the transgenic sequence does not contain intron insertions that could interfere with gene expression results. PCR cleanup of samples was performed using EdgeBio Quick Step 2 PCR purification kit following the manufactures protocol (Edge Biosystems, Gaithersburg, MD). Eluates were retained for sequencing.

Sequencing of PyMT transgene

Two Sanger sequencing reactions (one for each primer) were performed for the three samples using Big Dye chemistry (Applied Biosystems, Foster City, CA) following manufacturer's recommendations unless otherwise noted. Specifically, each 20 µL reaction contained 1.0ul of Big Dye version 3.1, 0.5ul of primer (10 mM of either PYVT1 or PYVT2) and 5ul of PCR cleaned product. Chain termination PCR was performed for 50 cycles. Products were purified of excess primers and dNTPS using Edge Bio Performa Gel Filtration Cartridge (Edge Biosystems, Gaithersburg, MD) and

detected using an Applied Biosystem 3730 DNA Analyzer (Applied Biosystems, Foster City, CA). Sequences were visualized and assembled using the Sequencher Version 5.2.4 (http://www.genecodes.com). Genomic and cDNA sequences aligned as expected and these sequence data were utilized to design RT-qPCR primers.

Real-time quantitative PCR

Gonadal adipose tissue and mammary gland was homogenized under liquid nitrogen using a polytron, and total RNA was extracted using chloroform and the E.Z.N.A. Total RNA Kit II (Omega Bio-tek, Norcross, GA) (192). Quantification of gonadal adipose tissue mRNA gene expression for macrophage markers (F4/80 and CD11c) and the adrenal enzyme Cyp19A1 (aromatase), mammary gland mRNA expression of macrophage markers (F4/80, CD11c and Mertk), inflammatory markers (MCP-1, IL-6, and TNFα), markers of angiogenesis (Vegfα, MMP2 and MMP9), and proliferation (Ki67) were performed as previously described (Applied Biosystems, Foster City, CA) (138). Quantification of mammary gland expression of the PyMT transgene was performed using a custom designed assay with forward primer: GGGCGGGTCTGAGTCCAT, reverse primer: AAATGAGCCCTCTGCAAATCC, and fluorescent probe: GGGAGGGTCTGATTCTTCG. Primers designed using the program Primer Express 3.0.1 (Applied Biosystems, Foster City, CA). Murine 18s rRNA was used as the housekeeping gene to normalize all of the data obtained. Quantitative reverse transcriptase polymerase chain reaction analysis was carried out as per the manufacturer's instructions and all primers used were TaqMan Gene Expression Assays (Applied Biosystems, Foster City, CA). Quantification of mRNA expression of all target genes was calculated using the $2\Delta\Delta C_T$ method.

Statistical analysis

All data were analyzed using commercial software (GraphPad Software, Prism 7, La Jolla, CA, USA). For Exp1, total body weight was analyzed using a two-way analysis of variance at each time point. Total visceral fat weight, total gonadal fat weight, mRNA analysis of gonadal fat F4/80, mammary gland inflammation and proliferation mediators and VEGFα were analyzed using a two-way analysis of variance. All DEXA information, sacrifice tumor data, mRNA analysis of gonadal fat CD11c, CD64, Cy19A1, mammary gland mRNA analysis of MMP2/9 were analyzed using a two tailed t-test. Bonferroni correction was used for all post-hoc analyses. In Exp2, all data was analyzed using a two tailed t-test. Statistical significance was set with an α value of $P \leq 0.05$. Data are represented as mean ± SEM.

*4.3 Results*

PyMT and wild-type mice fed a HFD have increased body weight gain and larger total visceral fat pad weight than mice fed a LFD

The HFD treatment significantly increased body weight for both the WT and PyMT groups beginning at 8 weeks of diet treatment and remained elevated through the 16-week treatment period (Figure 4.1A, $P<0.05$). A similar main effect of diet was observed for the total absolute weight of the visceral fat pads, with the HFD-fed mice having significantly greater total weight (Figure 4.1B, $P<0.05$). There was no difference between the HFD-treated groups for bodyweight (Figure 4.1A) and total visceral fat pad weight (Figure 4.1B). Body composition analysis for the WT mice at week 16 of treatment indicated that the mice fed the HFD had significantly greater body fat weight in

grams and body fat percentage (Figure 4.1C, D) with no difference for lean mass in grams between diet treatment groups (Figure 4.1E, $P<0.05$).

Chronic consumption of a HFD diet increases tumorigenesis and histopathological tumor stage progression in a premenopausal model

Chronic consumption of a HFD significantly increased primary mammary tumor growth and multiplicity with the mean tumor volume/mouse (Figure 4.2A) and mean tumor number/mouse (Figure 4.2B) determined at necropsy to be 1989±380 $mm^3$ and 8.85±0.96 for LFD, and 3163±542 $mm^3$ and 10.47±0.76 for HFD mice, respectively ($P<0.05$). HFD consumption significantly increased tumor burden (i.e. weight) (Figure 4.2C) with the mean/mouse to be 1599.7±206.9mg for LFD and 2554.0±375.4mg for HFD ($P<0.05$). Tumorigenesis in this model is classified into 4 distinct stages. Hyperplasia, the earliest change in the mammary gland, is characterized by clusters of densely packed lobules formed on the duct called the hyperplastic lesion. This change occurs around 4-6 weeks of age in this model and considering the age of the mice at sacrifice, it is understandable why we reported no samples in this early stage (Figure 4.2D). The next progressive stage is MIN (mammary intraepithelial neoplasia)/adenoma and describes a more florid epithelial proliferation still confined to the basement membrane of the duct, with minimal cytological atypia and no evidence of invasion or metastasis. In the current investigation, 40% of the samples classified in the low grade MIN/adenoma stage in the LFD-fed mice while zero mice from the HFD treated animals scored into this grade (Figure 4.2D). Progressively more advanced and considered the initial stage of malignant transition is the Early Carcinoma classification characterized by great cytological atypia and the

identification of early stromal invasion. The tumor cells now appear pleomorphic, showing moderate variation in nuclear morphology, size and shape and the majority of ducts are still morphologically normal, except for focal areas in which there is mild ductal epithelial hyperplasia with a small increase in the number of cell layers. We report no difference between the percentage of animals from each group that scored into this Early Invasive Carcinogenesis (40% for each group) stage (Figure 4.2D). Late Carcinoma is classified as poorly differentiated invasive ductal carcinoma. Tissues are composed of solid sheets of epithelial cells with little to no remaining acinar structures visible. The malignant cells in the tumor have marked variation in cellular and nuclear size and shape with vesicular nuclei and prominent nucleoli. We report 20% of the LFD-treated animals progressed to Late Carcinoma, however, 60% of the HFD treated mice classified into this advanced invasive carcinoma stage, (Figure 4.2D). Figure 4.2E illustrates a representative H/E stained sample from the LFD/Early Invasive and a HFD/Late Advanced Invasive stages. Given that tumorigenesis in this murine PyMT model is initially driven by the expression of the polyoma virus middle T oncoprotein, we wanted to establish that the expression of the transgene itself is not affected by diet manipulation, thus resulting in increased tumorigenesis due to differences in transgene expression. In this current experiment, diet treatment does not alter expression levels of the transgene as both experiment groups report similar mRNA expression levels (Figure 4.2F).

HFD intake leads to expansion of gonadal fat pad weight and increases aromatase expression and macrophage infiltration into the adipose tissue regardless of genotype

A significant main effect of diet was observed in the gonadal fat pad of the HFD-treated groups (Figure 4.3A, $P<0.05$). Cytochrome p50 aromatase (CyP19) mRNA expression was significantly elevated in the gonadal adipose tissue of the HFD-fed mice compared to the LFD-fed mice (Figure 4.3B, $P<0.05$). A significant main effect of diet was observed for macrophage markers F4/80 and CD11c expression in the adipose tissue (Figure 4.3C, $P<0.05$).

Tumorigenesis increases inflammatory and proliferation markers in the mammary gland

There was no difference in the mRNA expression of macrophage markers (F4/80 and CD64) between the LFD and HFD cancer groups in the mammary gland. However, HFD-feedings resulted in an upward trend in the expression of the macrophage marker Mertk in the mammary gland (Figure 4.3D, $p=0.06$). A significant genotype effect was observed in the mRNA expression of inflammatory cytokine and chemokine markers (IL-6, TNFα, and MCP-1), and the proliferation marker Ki67 of the mammary gland (Figure 4.3E, $P<0.05$). A main effect of both diet and genotype was observed for the angiogenic marker Vegfα. No significant difference in the gene expression of the matrix metalloproteinases (MMP2 and MMP9) was observed between cancer groups in the mammary gland ($P<0.05$) (Figure 4.3F).

Long-term HFD feedings drastically increases bodyweight gain for ovariectomized mice resulting in significant increases in total visceral fat weights over LFD-fed mice

The HFD treatment significantly (over 2 fold) increased body weight for ovariectomized mice beginning with the first week of diet treatment and remained elevated through the

18-week treatment period (Figure 4.4A, $P<0.05$). A similar main effect of diet was observed for the total absolute weight of the visceral fat pads (3 fold), with the HFD-fed mice having significantly greater total weight (Figure 4.4B, $P<0.05$).

Diet treatments had no effect on tumorigenesis in ovariectomized mice

HFD-induced obesity resulted in no significant change in tumor volume (Figure 4.5A), tumor number (Figure 4.5B), nor tumor weight (Figure 4.5C) between diet treatment groups. In fact, only a small percentage of mice from each group, 25% and 20% for LFD and HFD-fed mice from each group respectively, reported histopathological mammary gland stage progression into the MIN grade or beyond (Figure 4.5D). This is surprising given the analysis was performed at 24 weeks of age, an age well characterized into MIN/late advanced adenocarcinoma (191).

*4.4 Discussion*

Breast carcinomas continue to be the most commonly occurring cancer in women and the second leading cause of cancer-related deaths. Multiple molecular changes arising as a consequence of increased amounts of body fat are likely to contribute to the rising incidence of breast cancer and worse outcomes in the obese population; however, the exact mechanisms driving this relationship have not yet been fully elucidated. We examined mammary tumorigenesis in response to HFD feedings in the PyMT/MMTV transgenic murine model of tumorigenesis, an experimental model that presents morphological similarities with human breast carcinoma. This was done using both ovary-intact and ovariectomized mice in order to examine the influence of menopausal status on this response. Results show that ovary-intact mice fed a HFD not only have large increases in body weight gain and absolute visceral fat pad weight, but also have

significant proneoplastic effects on tumorigenesis as demonstrated by increases in primary tumor volume, tumor multiplicity, and total primary tumor burden (i.e. weight). Consistent with the tumor data, histopathology in the mammary gland of ovary-intact mice show an increase in histopathological stage progression with HFD-induced obesity. HFD treatment of intact mice also led to significant increases in aromatase and macrophage marker (F4/80 and CD11c) mRNA expression in the gonadal adipose tissue and an increasing trend of the macrophage cell marker Mertk expression in the mammary gland. However, we report no significant difference between diet treatment groups for localized inflammatory mediator mRNA expression, suggesting that localized inflammation in the mammary gland is not responsible for driving the HFD-induced increases in tumorigenesis seen in this model. HFD treatment in ovariectomized PyMT mice results in large increases in adiposity but has no significant effect on tumorigenesis, contrary to what we report in the ovary-intact mice. These data provide evidence that HFD-induced obesity exacerbates tumorigenesis in the HP PyMT/MMTV breast cancer model, which is associated with increases in aromatase. However, this response appears to be differentially dependent on menopausal status.

Breast cancer is a uniquely heterogeneous disease with different biological and clinical patterns between younger and older women. Thus, menopausal status as a prognostic factor becomes a topic of scrutiny. Differential associations have been identified according to menopausal status as there is clear evidence to support an increased breast cancer risk as a function of increasing BMI in postmenopausal women (78-95); however, studies in premenopausal women are more controversial. Our results are consistent with previous epidemiological studies, such as Chang *et al.,* that have

reported that obesity is significantly associated with increasing risk of breast cancer in a patient population that were more likely to be premenopausal (76). Similarly, Nagrani *et al.,* concluded that central obesity is a risk factor for breast cancer irrespective of menopausal status (73). However, relatively few mechanistic studies investigating obesity and breast cancer progression in premenopausal animal models have been performed. Contradictory to published studies that have determined a positive correlation between obesity and breast cancer risk in a postmenopausal model, our data demonstrates no significant effect of HFD-induced obesity on breast cancer progression in this murine model. This is surprising considering there is overwhelming data to suggest that obese postmenopausal women are at significantly increased risk of developing HP breast cancer. With obesity, ER+ and PR+ hormone-dependent breast cancers are of importance as estrogen signaling is likely to be a key contributor to obesity-associated breast cancer. Importantly, activation of ERα-dependent gene expression as a consequence of adipose inflammation has been observed in murine mammary fat pads and human breast samples (68, 97, 98).

The primary site for estrogen biosynthesis in premenopausal women is the ovary but other peripheral sources have increased relative importance in estrogen synthesis. For instance, adipose tissue expresses the estrogen synthase cytochrome aromatase p450 (100, 101), which is encoded by the *Cyp19* gene, and contributes to estrogen synthesis. In postmenopausal women, obesity and associated inflammation have been shown to contribute to increased breast cancer risk as the adipose tissue is the primary source of estrogen synthesis due to increased aromatase expression (102-104). In support of this concept, studies link aromatase expression in inflamed adipose tissue of obese women

with the upregulation of proinflammatory mediators, such as macrophages, as aromatase transcription can be induced by the interaction of inflammatory cytokines with their receptors. Our data is consistent with this concept in that ovary-intact mice fed a HFD have significant increases in aromatase expression in the gonadal adipose tissue. We show that increased aromatase expression is associated with increases in certain macrophage markers and increases in not only primary tumor growth but also histopathological grade of the mammary gland in obesity-induced ovary-intact mice. Thus, it is likely that paracrine interactions between macrophages and other cell types operate on an inflammatory axis that results in elevated estrogen biosynthesis and expression; however, further delineation of this axis is required before treatment mechanisms can be established.

There are several limitations to our study pertaining to the ovariectomized postmenopausal model that warrant cautious interpretations of the findings. We designed this study to replicate a mouse model where we could exclusively look at the role of adipose tissue aromatase expression on mammary tumor initiation and progression without the effect of endogenous estrogen and progesterone. However, tumorigenesis in this model appears to be highly dependent on these endogenous hormones and removing the ovaries at 5 weeks of age may have interfered with tumor initiation in these mice, thus the relatively low tumor number in the ovariectomized versus the ovary intact mice. Another potential limitation is the effect that the removal of the ovaries had on normal mammary gland development. Literature suggests that estrogen is circulating in female mice at 4 weeks of age but progesterone is not bioavailable until 7 weeks of age or even sexual maturation which occurs around 8 weeks of age. Bocchinfuso *et al.*, demonstrated

that without functioning estrogen and progesterone, normal mammary gland development does not occur (193). Given that we ovariectomized these mice at 5 weeks of age, we cannot establish that decreases in tumor initiation in the ovariectomized mice was due to decreases in bioavailable estrogen or immature mammary gland development. For future studies, it may be beneficial to wait to remove the ovaries until sexual maturation occurs. However, it should be noted that by this time point this mouse model would have progressed into the MIN histopathological tumor stage; thus, analysis of obesity-induced pathologies would be on tumor progression rather than tumor initiation. Given, the amount of time it takes for increased adiposity to occur in a HFD-induced obesity model, this represents a challenge as this transgenic model produces tumorigenesis in a relatively short time frame.

In summary, we report that HFD-induced obesity results in increases in mammary tumorigenesis and upregulated aromatase expression in the gonadal adipose tissue in the HP PyMT/MMTV murine model of premenopausal breast cancer. Although, aromatase expression has been implicated in modulating multiple mechanisms in postmenopausal breast cancer, its involvement in tumorigenesis in a premenopausal model has not been established. While it is well known that obesity leads to increased levels of proinflammatory mediators, further research is required to demonstrate the functional link of increased aromatase expression in mammary tumorigenesis. This newly discovered obesity, inflammation, and aromatase axis provides the basis for developing mechanism-based strategies to reduce the risk of HP breast cancer in this growing segment of the population.

*4.5 Figures & Legends*

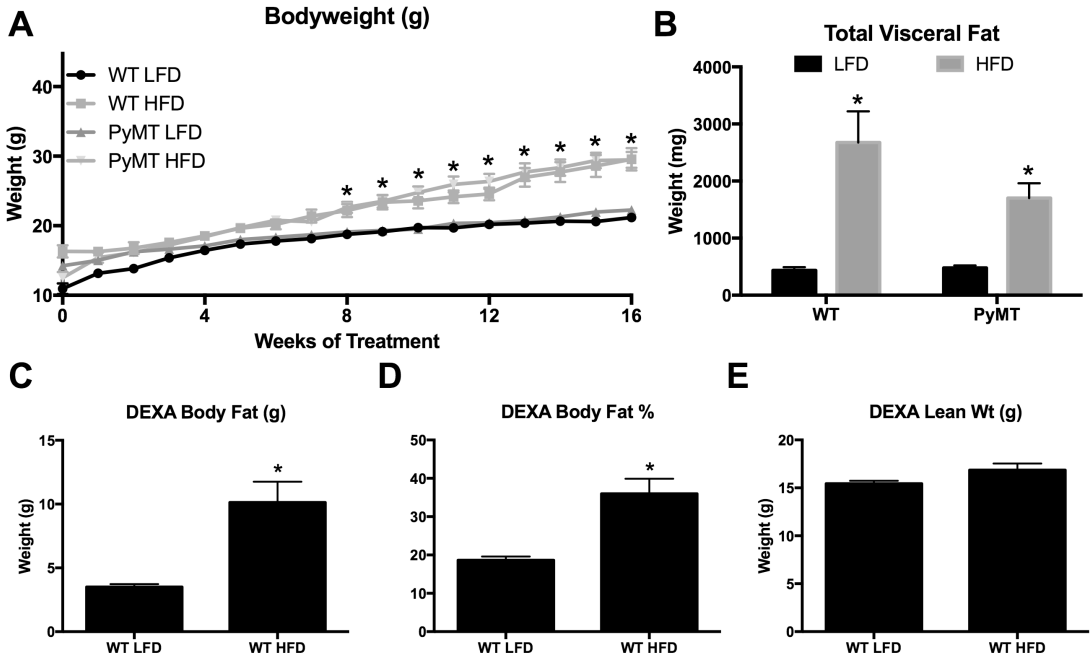


Figure 4.1:

Body weight characteristics for Exp1. A. Body weight in grams. B. Total absolute weight of visceral fat pads. C. Body composition analysis of WT mice, Body fat in grams. D. Body fat percentage. E. Lean weight in grams. *main effect of diet. Data are represented as ± SEM, n=7 WT LFD, n=8 WT HFD, n=8 PyMT LFD, n=12 PyMT HFD, n=15.

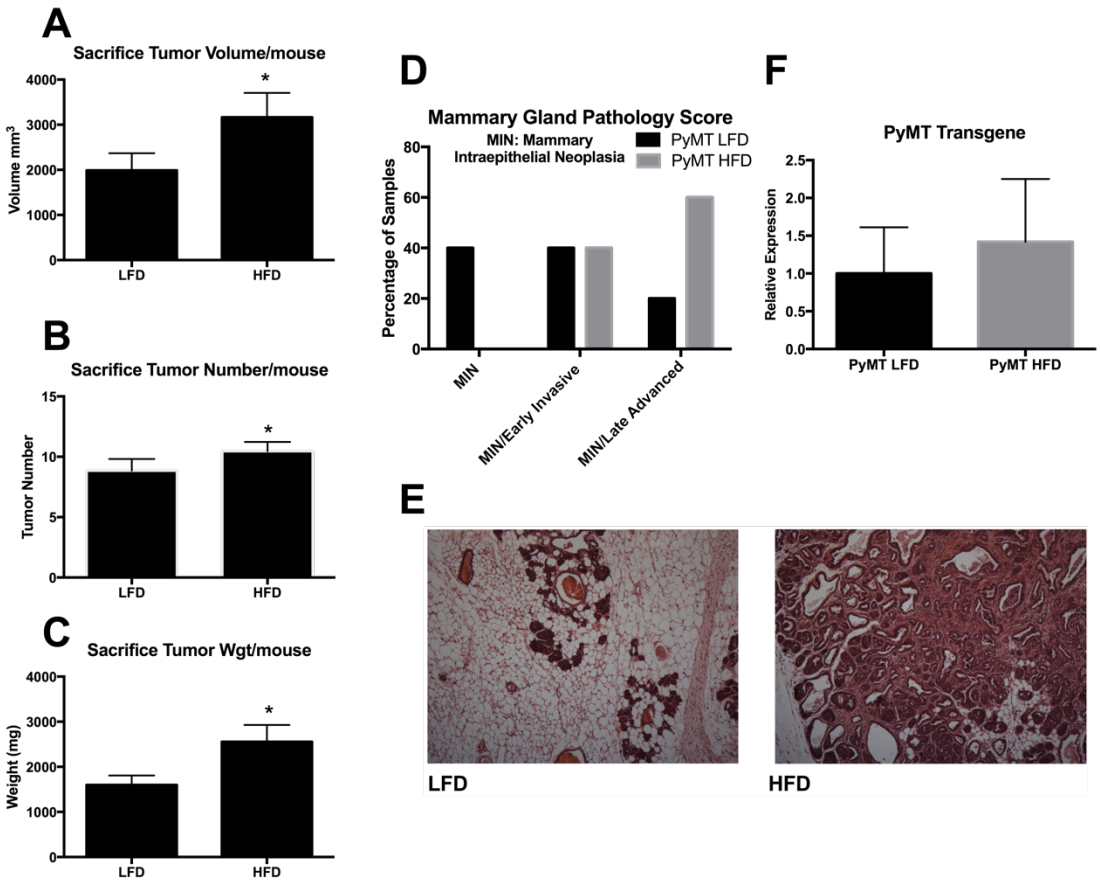


Figure 4.2:

Sacrifice tumor and histopathology scoring for Exp1. A. Sacrifice tumor volume per mouse. B. Sacrifice tumor number per mouse. C. Sacrifice tumor burden (weight) per mouse. D. Mammary gland histopathology scoring for both treatment groups. E. Representative images from each treatment group of the most frequently reported stage in each group. F. mRNA expression of the PyMT transgene in the mammary gland. *P<0.05. Data are represented as ± SEM, PyMT LFD, n=12 PyMT HFD, n=15.

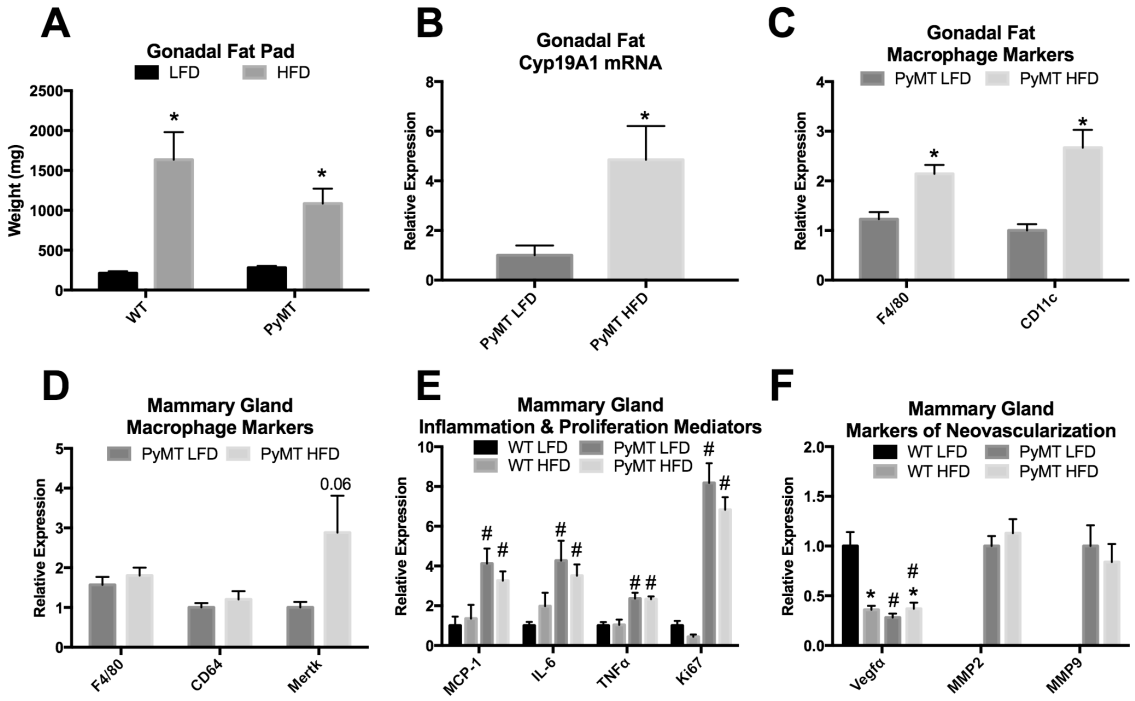


Figure 4.3

Markers of inflammation in the gonadal fat and mammary gland. A. Total gonadal fat weights for each treatment group. B. Aromatase mRNA gene expression for cancer groups in the gonadal fat. C. mRNA expression of macrophage marker F4/80 and CD11c in gonadal fat. D. mRNA expression of macrophage marker F4/80, CD11c, Mertk in mammary gland. E. Markers of inflammation and proliferation in the mammary gland to include MCP-1, IL-6, TNFα, Ki67. F. Markers of neovascularization in the mammary gland to include Vegfα, MMP2/9. *main effect of diet, #main effect of genotype. Data are represented as ± SEM, WT LFD, n=8 WT HFD, n=8 PyMT LFD, n=12 PyMT HFD, n=15.

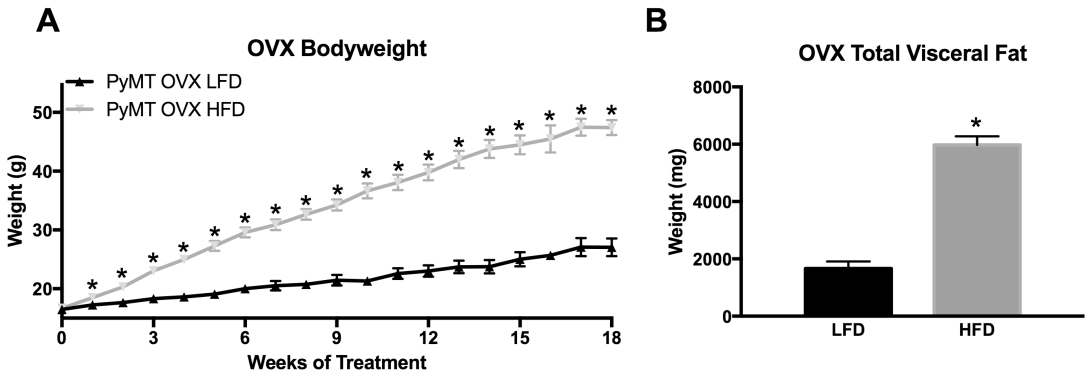


Figure 4.4

Bodyweight characteristics for Exp2. A. Body weight in grams. B. Total absolute visceral fat pad weight. *P<0.05. Data are represented as ± SEM, PyMT OVX LFD, n=9 PyMT OVX HFD, n=12.

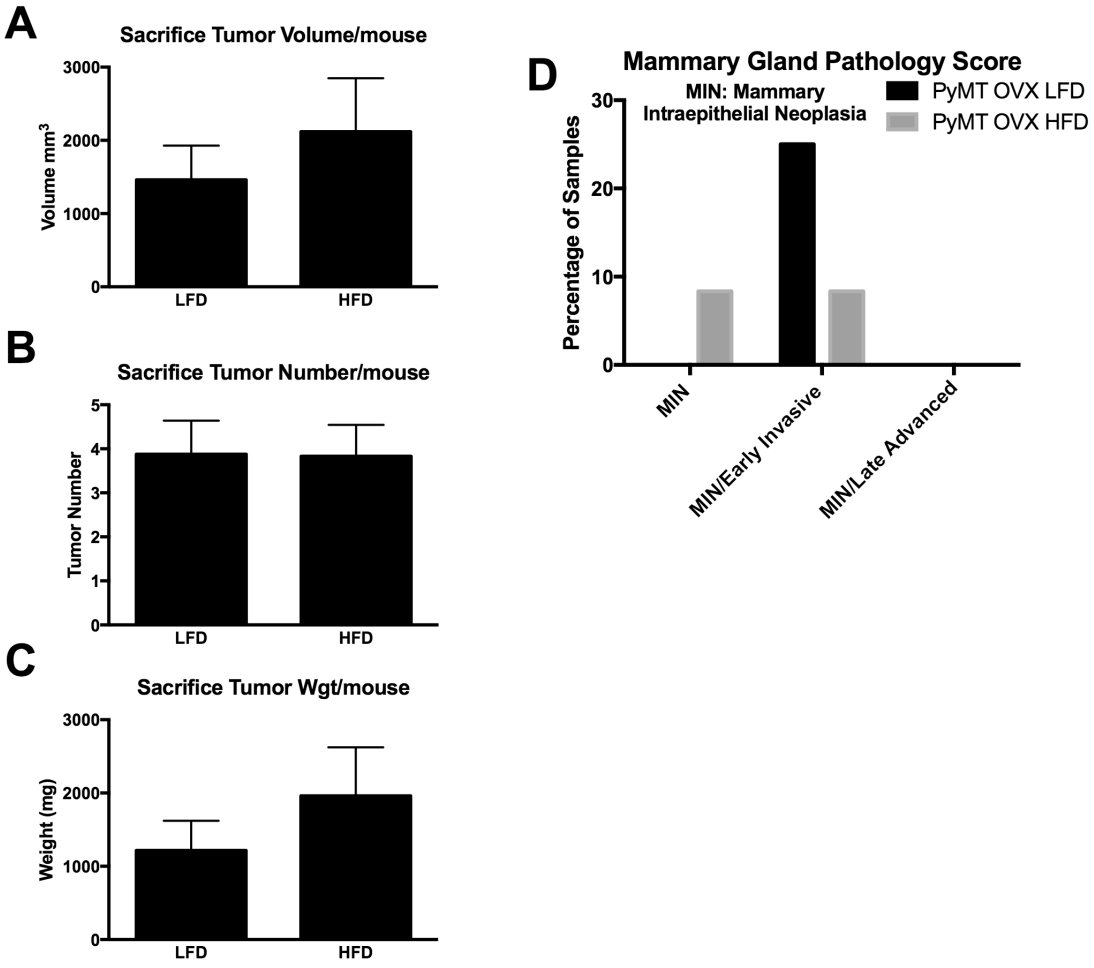


Figure 4.5:

Sacrifice tumor and histopathology scoring for Exp2. A. Sacrifice tumor volume per mouse. B. Sacrifice tumor number per mouse. C. Sacrifice tumor burden (weight) per mouse. D. Mammary gland histopathology scoring for both treatment groups. *P<0.05. Data are represented as ± SEM, PyMT OVX LFD, n=9 PyMT OVX HFD, n=12.

# CHAPTER 5

# SUMMARY AND CONCLUSIONS

Obesity is now considered to be a modern epidemic and its strong association with insulin resistance and chronic inflammation has elicited interest in the underlying mechanisms of these pathologies. Adipose tissue inflammation is causally associated with obesity-related metabolic disorders and macrophages are known to be major players in these processes. What is less well recognized is the fact that obesity is associated with increased risk of a number of cancers, including those of the colon, endometrium and the breast. In these aforementioned studies, we tested the central hypothesis that chronic inflammation plays a critical role in the progression and severity of obesity-induced insulin resistance and hormone-dependent breast cancer progression. Additionally, we examined the role of MCP-1 expression in an obesogenic inflammatory environment and furthermore, the association of this chemokine with mammary tumorigenesis.

Overwhelming evidence suggests adipose tissue macrophages participate in obesity-related complications given their propensity to promote inflammation in the adipose tissue. In our first study, we examined the role of the macrophage chemokine, MCP-1, on the inflammatory processes associated with high fat diet-induced obesity. However contrary to our hypothesis, MCP-1 depletion contributed to increases in macrophage accumulation, increases in adiposity as well as increases in insulin resistance and altered glucose sensitivity. As such, we reported a protective role of MCP-1 in the adipose tissue in response to HFD feedings. Given the ambiguous findings of the role of MCP-1 in various studies involving obesity-related perturbations, more research is needed to fully ascertain the role of this chemokine in this processes.

Breast cancer is the second leading killer among women worldwide, as such, the need to identify novel therapeutic targets is crucial. Clinical studies implicate MCP-1 as

a major modulator in the progression of mammary tumorigenesis. Macrophages are key mediators in the connection between inflammation and cancer progression; demonstrated by the role of MCP-1 as a powerful macrophage chemoattractant. To examine the effect of MCP-1 in the development and progression of mammary tumorigenesis, we developed an MCP-$1^{-/-}$ transgenic triple negative breast cancer model. Genetic deletion of MCP-1 expression resulted in decreased tumorigenesis; indicated by decreases in primary tumor volume and multiplicity, but also a delay in tumor progression demonstrated through histopathology scoring of the mammary gland. Ablation of MCP-1 expression also resulted in decreases of inflammatory mediator expression in the localized and tumor microenvironment. It is known that MCP-1 represents a causal connection between inflammation and macrophage recruitment and not surprisingly, therefore has an emergent role in the development of mammary tumorigenesis. However, more research is required to fully understand the importance and function of MCP-1 in a triple negative breast cancer microenvironment.

Given that two out of three women in the United States are overweight or obese, an understanding of the mechanisms that link obesity to breast cancer, and the connection with menopausal status, is of critical public health importance. There is powerful evidence that implicates obesity-associated adipose tissue inflammation and aromatase expression are critically linked. In our final study, we examined mammary tumorigenesis in response to HFD feedings in a hormone receptor positive model of breast cancer, a model that closely resembles the etiology of human breast carcinoma. This was done using both ovary-intact and ovariectomized mice in order to examine the influence of menopausal status on this response. Results show that HFD-induced obesity exacerbates

tumorigenesis in the premenopausal model indicated by significant proneoplastic effects (i.e. primary tumor volume, multiplicity, weight) and advances in histopathological grade of the mammary gland. HFD treatment of intact mice also led to significant increases in aromatase and macrophage marker mRNA expression in the gonadal adipose tissue and an increasing trend of mRNA expression of a macrophage marker in the mammary gland. HFD feedings in ovariectomized PyMT mice resulted in large increases in adiposity but had no significant effect on tumorigenesis. This is not only contrary to what we report in the ovary-intact mice but also surprising considering the amount of literature that suggests obese postmenopausal women are at a significant increased risk of breast cancer. Although, aromatase expression has been implicated in modulating multiple mechanisms in postmenopausal breast cancer, its involvement in tumorigenesis in a premenopausal model has not been established; thus further research is needed before mechanism-based strategies can be established.

The prevalence of obesity is rapidly increasing worldwide; thus so are obesity-associated cancer rates. Understanding the pleotropic effects of chronic inflammation represents a challenging problem. However, gaining increased understanding of the relationship between inflammation – obesity – and cancer can provide novel insight into the development of mechanism-based therapeutic strategies.

# REFERENCES


1.Roberts DL, Dive C, Renehan AG. Biological mechanisms linking obesity and cancer risk: new perspectives. Annu Rev Med. 2010;61:301-16.
2.Basen-Engquist K, Chang M. Obesity and cancer risk: recent review and evidence. Curr Oncol Rep. 2011;13(1):71-6.
3.Kahn SE, Hull RL, Utzschneider KM. Mechanisms linking obesity to insulin resistance and type 2 diabetes. Nature. 2006;444(7121):840-6.
4.Ozcan U, Cao Q, Yilmaz E, Lee AH, Iwakoshi NN, Ozdelen E, et al. Endoplasmic reticulum stress links obesity, insulin action, and type 2 diabetes. Science. 2004;306(5695):457-61.
5.Olefsky JM, Glass CK. Macrophages, inflammation, and insulin resistance. Annu Rev Physiol. 2010;72:219-46.
6.Ungefroren H, Gieseler F, Fliedner S, Lehnert H. Obesity and cancer. Horm Mol Biol Clin Investig. 2015;21(1):5-15.
7.Fox KR, Hillsdon M. Physical activity and obesity. Obes Rev. 2007;8 Suppl 1:115-21.
8.Wareham NJ, van Sluijs EM, Ekelund U. Physical activity and obesity prevention: a review of the current evidence. Proc Nutr Soc. 2005;64(2):229-47.
9.Lemmens VE, Oenema A, Klepp KI, Henriksen HB, Brug J. A systematic review of the evidence regarding efficacy of obesity prevention interventions among adults. Obes Rev. 2008;9(5):446-55.
10.Greenberg AS, Obin MS. Obesity and the role of adipose tissue in inflammation and metabolism. Am J Clin Nutr. 2006;83(2):461S-5S.
11.Shoelson SE, Lee J, Goldfine AB. Inflammation and insulin resistance. J Clin Invest. 2006;116(7):1793-801.
12.Guilherme A, Virbasius JV, Puri V, Czech MP. Adipocyte dysfunctions linking obesity to insulin resistance and type 2 diabetes. Nat Rev Mol Cell Biol. 2008;9(5):367-77.
13.Aouadi M, Tencerova M, Vangala P, Yawe JC, Nicoloro SM, Amano SU, et al. Gene silencing in adipose tissue macrophages regulates whole-body metabolism in obese mice. Proc Natl Acad Sci U S A. 2013;110(20):8278-83.
14.Weisberg SP, McCann D, Desai M, Rosenbaum M, Leibel RL, Ferrante AW, Jr. Obesity is associated with macrophage accumulation in adipose tissue. J Clin Invest. 2003;112(12):1796-808.
15.Gregoire FM, Smas CM, Sul HS. Understanding adipocyte differentiation. Physiol Rev. 1998;78(3):783-809.
16.Sethi JK, Vidal-Puig AJ. Thematic review series: adipocyte biology. Adipose tissue function and plasticity orchestrate nutritional adaptation. J Lipid Res. 2007;48(6):1253-62.

17.McArdle MA, Finucane OM, Connaughton RM, McMorrow AM, Roche HM. Mechanisms of obesity-induced inflammation and insulin resistance: insights into the emerging role of nutritional strategies. Front Endocrinol (Lausanne). 2013;4:52
18.Gual P, Le Marchand-Brustel Y, Tanti JF. Positive and negative regulation of insulin signaling through IRS-1 phosphorylation. Biochimie. 2005;87(1):99-109.
19.Curat CA, Miranville A, Sengenes C, Diehl M, Tonus C, Busse R, et al. From blood monocytes to adipose tissue-resident macrophages: induction of diapedesis by human mature adipocytes. Diabetes. 2004;53(5):1285-92.
20.Verstrepen L, Bekaert T, Chau TL, Tavernier J, Chariot A, Beyaert R. TLR-4, IL-1R and TNF-R signaling to NF-kappaB: variations on a common theme. Cell Mol Life Sci. 2008;65(19):2964-78.
21.Shoelson SE, Lee J, Yuan M. Inflammation and the IKK beta/I kappa B/NF-kappa B axis in obesity- and diet-induced insulin resistance. Int J Obes Relat Metab Disord. 2003;27 Suppl 3:S49-52.
22.Bruning U, Fitzpatrick SF, Frank T, Birtwistle M, Taylor CT, Cheong A. NFkappaB and HIF display synergistic behaviour during hypoxic inflammation. Cell Mol Life Sci. 2012;69(8):1319-29.
23.Deshmane SL, Kremlev S, Amini S, Sawaya BE. Monocyte chemoattractant protein-1 (MCP-1): an overview. J Interferon Cytokine Res. 2009;29(6):313-26.
24.Hemmerich S, Paavola C, Bloom A, Bhakta S, Freedman R, Grunberger D, et al. Identification of residues in the monocyte chemotactic protein-1 that contact the MCP-1 receptor, CCR2. Biochemistry. 1999;38(40):13013-25.
25.Han KH, Green SR, Tangirala RK, Tanaka S, Quehenberger O. Role of the first extracellular loop in the functional activation of CCR2. The first extracellular loop contains distinct domains necessary for both agonist binding and transmembrane signaling. J Biol Chem. 1999;274(45):32055-62.
26.Brown MA, Hural J. Functions of IL-4 and control of its expression. Crit Rev Immunol. 1997;17(1):1-32.
27.Cushing SD, Berliner JA, Valente AJ, Territo MC, Navab M, Parhami F, et al. Minimally modified low density lipoprotein induces monocyte chemotactic protein 1 in human endothelial cells and smooth muscle cells. Proc Natl Acad Sci U S A. 1990;87(13):5134-8.
28.Barna BP, Pettay J, Barnett GH, Zhou P, Iwasaki K, Estes ML. Regulation of monocyte chemoattractant protein-1 expression in adult human non-neoplastic astrocytes is sensitive to tumor necrosis factor (TNF) or antibody to the 55-kDa TNF receptor. J Neuroimmunol. 1994;50(1):101-7.
29.Yoshimura T, Robinson EA, Tanaka S, Appella E, Leonard EJ. Purification and amino acid analysis of two human monocyte chemoattractants produced by phytohemagglutinin-stimulated human blood mononuclear leukocytes. J Immunol. 1989;142(6):1956-62.
30.Harman-Boehm I, Bluher M, Redel H, Sion-Vardy N, Ovadia S, Avinoach E, et al. Macrophage infiltration into omental versus subcutaneous fat across different populations: effect of regional adiposity and the comorbidities of obesity. J Clin Endocrinol Metab. 2007;92(6):2240-7.

31.Huber J, Kiefer FW, Zeyda M, Ludvik B, Silberhumer GR, Prager G, et al. CC chemokine and CC chemokine receptor profiles in visceral and subcutaneous adipose tissue are altered in human obesity. J Clin Endocrinol Metab. 2008;93(8):3215-21.
32.Lodi PJ, Garrett DS, Kuszewski J, Tsang ML, Weatherbee JA, Leonard WJ, et al. High-resolution solution structure of the beta chemokine hMIP-1 beta by multidimensional NMR. Science. 1994;263(5154):1762-7.
33.Loetscher P, Seitz M, Baggiolini M, Moser B. Interleukin-2 regulates CC chemokine receptor expression and chemotactic responsiveness in T lymphocytes. J Exp Med. 1996;184(2):569-77.
34.Sozzani S, Zhou D, Locati M, Rieppi M, Proost P, Magazin M, et al. Receptors and transduction pathways for monocyte chemotactic protein-2 and monocyte chemotactic protein-3. Similarities and differences with MCP-1. J Immunol. 1994;152(7):3615-22.
35.Mellado M, Rodriguez-Frade JM, Aragay A, del Real G, Martin AM, Vila-Coro AJ, et al. The chemokine monocyte chemotactic protein 1 triggers Janus kinase 2 activation and tyrosine phosphorylation of the CCR2B receptor. J Immunol. 1998;161(2):805-13.
36.Turner SJ, Domin J, Waterfield MD, Ward SG, Westwick J. The CC chemokine monocyte chemotactic peptide-1 activates both the class I p85/p110 phosphatidylinositol 3-kinase and the class II PI3K-C2alpha. J Biol Chem. 1998;273(40):25987-95.
37.Cambien B, Pomeranz M, Millet MA, Rossi B, Schmid-Alliana A. Signal transduction involved in MCP-1-mediated monocytic transendothelial migration. Blood. 2001;97(2):359-66.
38.Wain JH, Kirby JA, Ali S. Leucocyte chemotaxis: Examination of mitogen-activated protein kinase and phosphoinositide 3-kinase activation by Monocyte Chemoattractant Proteins-1, -2, -3 and -4. Clin Exp Immunol. 2002;127(3):436-44.
39.Gu L, Tseng SC, Rollins BJ. Monocyte chemoattractant protein-1. Chem Immunol. 1999;72:7-29.
40.Melgarejo E, Medina MA, Sanchez-Jimenez F, Urdiales JL. Monocyte chemoattractant protein-1: a key mediator in inflammatory processes. Int J Biochem Cell Biol. 2009;41(5):998-1001.
41.Ruiz-Ortega M, Lorenzo O, Egido J. Angiotensin III increases MCP-1 and activates NF-kappaB and AP-1 in cultured mesangial and mononuclear cells. Kidney Int. 2000;57(6):2285-98.
42.Cranford TL, Enos RT, Velazquez KT, McClellan JL, Davis JM, Singh UP, et al. Role of MCP-1 on inflammatory processes and metabolic dysfunction following high-fat feedings in the FVB/N strain. Int J Obes (Lond). 2016;40(5):844-51.
43.De Paepe B, Creus KK, De Bleecker JL. Chemokines in idiopathic inflammatory myopathies. Front Biosci. 2008;13:2548-77.
44.Cipollone F, Marini M, Fazia M, Pini B, Iezzi A, Reale M, et al. Elevated circulating levels of monocyte chemoattractant protein-1 in patients with restenosis after coronary angioplasty. Arterioscler Thromb Vasc Biol. 2001;21(3):327-34.
45.Dawson TC, Kuziel WA, Osahar TA, Maeda N. Absence of CC chemokine receptor-2 reduces atherosclerosis in apolipoprotein E-deficient mice. Atherosclerosis. 1999;143(1):205-11.
46.O'Hayre M, Salanga CL, Handel TM, Allen SJ. Chemokines and cancer: migration, intracellular signalling and intercellular communication in the microenvironment. Biochem J. 2008;409(3):635-49.

47.Steiner JL, Davis JM, McClellan JL, Guglielmotti A, Murphy EA. Effects of the MCP-1 synthesis inhibitor bindarit on tumorigenesis and inflammatory markers in the C3(1)/SV40Tag mouse model of breast cancer. Cytokine. 2014;66(1):60-8.
48.Ueno T, Toi M, Saji H, Muta M, Bando H, Kuroi K, et al. Significance of macrophage chemoattractant protein-1 in macrophage recruitment, angiogenesis, and survival in human breast cancer. Clin Cancer Res. 2000;6(8):3282-9.
49.Lee J. Adipose tissue macrophages in the development of obesity-induced inflammation, insulin resistance and type 2 diabetes. Arch Pharm Res. 2013;36(2):208-22.
50.Suganami T, Ogawa Y. Adipose tissue macrophages: their role in adipose tissue remodeling. J Leukoc Biol. 2010;88(1):33-9.
51.Enos RT, Davis JM, Velazquez KT, McClellan JL, Day SD, Carnevale KA, et al. Influence of dietary saturated fat content on adiposity, macrophage behavior, inflammation, and metabolism: composition matters. Journal of lipid research. 2013;54(1):152-63.
52.Gerhardt CC, Romero IA, Cancello R, Camoin L, Strosberg AD. Chemokines control fat accumulation and leptin secretion by cultured human adipocytes. Mol Cell Endocrinol. 2001;175(1-2):81-92.
53.Cancello R, Henegar C, Viguerie N, Taleb S, Poitou C, Rouault C, et al. Reduction of macrophage infiltration and chemoattractant gene expression changes in white adipose tissue of morbidly obese subjects after surgery-induced weight loss. Diabetes. 2005;54(8):2277-86.
54.Xu H, Barnes GT, Yang Q, Tan G, Yang D, Chou CJ, et al. Chronic inflammation in fat plays a crucial role in the development of obesity-related insulin resistance. J Clin Invest. 2003;112(12):1821-30.
55.Cancello R, Tordjman J, Poitou C, Guilhem G, Bouillot JL, Hugol D, et al. Increased infiltration of macrophages in omental adipose tissue is associated with marked hepatic lesions in morbid human obesity. Diabetes. 2006;55(6):1554-61.
56.Harkins JM, Moustaid-Moussa N, Chung YJ, Penner KM, Pestka JJ, North CM, et al. Expression of interleukin-6 is greater in preadipocytes than in adipocytes of 3T3-L1 cells and C57BL/6J and ob/ob mice. J Nutr. 2004;134(10):2673-7.
57.Gordon S, Taylor PR. Monocyte and macrophage heterogeneity. Nat Rev Immunol. 2005;5(12):953-64.
58.Mantovani A, Sica A, Sozzani S, Allavena P, Vecchi A, Locati M. The chemokine system in diverse forms of macrophage activation and polarization. Trends Immunol. 2004;25(12):677-86.
59.Wang N, Liang H, Zen K. Molecular mechanisms that influence the macrophage m1-m2 polarization balance. Front Immunol. 2014;5:614.
60.Fujisaka S, Usui I, Bukhari A, Ikutani M, Oya T, Kanatani Y, et al. Regulatory mechanisms for adipose tissue M1 and M2 macrophages in diet-induced obese mice. Diabetes. 2009;58(11):2574-82.
61.Lumeng CN, Bodzin JL, Saltiel AR. Obesity induces a phenotypic switch in adipose tissue macrophage polarization. J Clin Invest. 2007;117(1):175-84.
62.Kraakman MJ, Murphy AJ, Jandeleit-Dahm K, Kammoun HL. Macrophage polarization in obesity and type 2 diabetes: weighing down our understanding of macrophage function? Front Immunol. 2014;5:470.

63.Suganami T, Nishida J, Ogawa Y. A paracrine loop between adipocytes and macrophages aggravates inflammatory changes: role of free fatty acids and tumor necrosis factor alpha. Arterioscler Thromb Vasc Biol. 2005;25(10):2062-8.
64.Rose DP, Gracheck PJ, Vona-Davis L. The Interactions of Obesity, Inflammation and Insulin Resistance in Breast Cancer. Cancers (Basel). 2015;7(4):2147-68.
65.Protani M, Coory M, Martin JH. Effect of obesity on survival of women with breast cancer: systematic review and meta-analysis. Breast Cancer Res Treat. 2010;123(3):627-35.
66.Chlebowski RT, Aiello E, McTiernan A. Weight loss in breast cancer patient management. J Clin Oncol. 2002;20(4):1128-43.
67.Howe LR, Subbaramaiah K, Hudis CA, Dannenberg AJ. Molecular pathways: adipose inflammation as a mediator of obesity-associated cancer. Clin Cancer Res. 2013;19(22):6074-83.
68.Morris PG, Hudis CA, Giri D, Morrow M, Falcone DJ, Zhou XK, et al. Inflammation and increased aromatase expression occur in the breast tissue of obese women with breast cancer. Cancer Prev Res (Phila). 2011;4(7):1021-9.
69.Berstad P, Coates RJ, Bernstein L, Folger SG, Malone KE, Marchbanks PA, et al. A case-control study of body mass index and breast cancer risk in white and African-American women. Cancer Epidemiol Biomarkers Prev. 2010;19(6):1532-44.
70.Cheraghi Z, Poorolajal J, Hashem T, Esmailnasab N, Doosti Irani A. Effect of body mass index on breast cancer during premenopausal and postmenopausal periods: a meta-analysis. PLoS One. 2012;7(12):e51446.
71.Anderson GL, Neuhouser ML. Obesity and the risk for premenopausal and postmenopausal breast cancer. Cancer Prev Res (Phila). 2012;5(4):515-21.
72.Renehan AG, Tyson M, Egger M, Heller RF, Zwahlen M. Body-mass index and incidence of cancer: a systematic review and meta-analysis of prospective observational studies. Lancet. 2008;371(9612):569-78.
73.Nagrani R, Mhatre S, Rajaraman P, Soerjomataram I, Boffetta P, Gupta S, et al. Central obesity increases risk of breast cancer irrespective of menopausal and hormonal receptor status in women of South Asian Ethnicity. Eur J Cancer. 2016;66:153-61.
74.Schapira DV, Kumar NB, Lyman GH, Cox CE. Obesity and body fat distribution and breast cancer prognosis. Cancer. 1991;67(2):523-8.
75.Schapira DV, Kumar NB, Lyman GH. Obesity, body fat distribution, and sex hormones in breast cancer patients. Cancer. 1991;67(8):2215-8.
76.Chang S, Buzdar AU, Hursting SD. Inflammatory breast cancer and body mass index. J Clin Oncol. 1998;16(12):3731-5.
77.Loi S, Milne RL, Friedlander ML, McCredie MR, Giles GG, Hopper JL, et al. Obesity and outcomes in premenopausal and postmenopausal breast cancer. Cancer Epidemiol Biomarkers Prev. 2005;14(7):1686-91.
78.Calle EE, Kaaks R. Overweight, obesity and cancer: epidemiological evidence and proposed mechanisms. Nat Rev Cancer. 2004;4(8):579-91.
79.Patterson RE, Cadmus LA, Emond JA, Pierce JP. Physical activity, diet, adiposity and female breast cancer prognosis: a review of the epidemiologic literature. Maturitas.66(1):5-15.
80.Brown KA, Simpson ER. Obesity and breast cancer: progress to understanding the relationship. Cancer Res.70(1):4-7.

81.Cleary MP, Grossmann ME, Ray A. Effect of obesity on breast cancer development. Vet Pathol.47(2):202-13.
82.Amaral P, Miguel R, Mehdad A, Cruz C, Monteiro Grillo I, Camilo M, et al. Body fat and poor diet in breast cancer women. Nutr Hosp.25(3):456-61.
83.Wolin KY, Carson K, Colditz GA. Obesity and cancer. Oncologist.15(6):556-65.
84.Protani M, Coory M, Martin JH. Effect of obesity on survival of women with breast cancer: systematic review and meta-analysis. Breast Cancer Res Treat.
85.Dirat B, Bochet L, Escourrou G, Valet P, Muller C. Unraveling the obesity and breast cancer links: a role for cancer-associated adipocytes? Endocr Dev.19:45-52.
86.Hellmann SS, Thygesen LC, Tolstrup JS, Gronbaek M. Modifiable risk factors and survival in women diagnosed with primary breast cancer: results from a prospective cohort study. Eur J Cancer Prev.19(5):366-73.
87.Nagaiah G, Hazard HW, Abraham J. Role of obesity and exercise in breast cancer survivors. Oncology (Williston Park).24(4):342-6.
88.Baer HJ, Tworoger SS, Hankinson SE, Willett WC. Body fatness at young ages and risk of breast cancer throughout life. Am J Epidemiol.171(11):1183-94.
89.Stark A, Stahl MS, Kirchner HL, Krum S, Prichard J, Evans J. Body mass index at the time of diagnosis and the risk of advanced stages and poorly differentiated cancers of the breast: findings from a case-series study. Int J Obes (Lond).
90.Maccio A, Madeddu C, Gramignano G, Mulas C, Floris C, Massa D, et al. Correlation of body mass index and leptin with tumor size and stage of disease in hormone-dependent postmenopausal breast cancer: preliminary results and therapeutic implications. J Mol Med.88(7):677-86.
91.Chen X, Lu W, Zheng W, Gu K, Chen Z, Zheng Y, et al. Obesity and weight change in relation to breast cancer survival. Breast Cancer Res Treat.122(3):823-33.
92.Malin A, Matthews CE, Shu XO, Cai H, Dai Q, Jin F, et al. Energy balance and breast cancer risk. Cancer Epidemiol Biomarkers Prev. 2005;14(6):1496-501.
93.Thomson CA, Thompson PA. Dietary patterns, risk and prognosis of breast cancer. Future Oncol. 2009;5(8):1257-69.
94.Brown KA, Simpson ER. Obesity and breast cancer: mechanisms and therapeutic implications. Front Biosci (Elite Ed).4:2515-24.
95.Gross A, Newschaffer CJ, Hoffman Bolton JA, Rifai N, Visvanathan K. Adipocytokines, Inflammation, and Breast Cancer Risk in Postmenopausal Women: A prospective study. Cancer Epidemiol Biomarkers Prev.
96.Sorlie T, Tibshirani R, Parker J, Hastie T, Marron JS, Nobel A, et al. Repeated observation of breast tumor subtypes in independent gene expression data sets. Proc Natl Acad Sci U S A. 2003;100(14):8418-23.
97.Subbaramaiah K, Howe LR, Bhardwaj P, Du B, Gravaghi C, Yantiss RK, et al. Obesity is associated with inflammation and elevated aromatase expression in the mouse mammary gland. Cancer Prev Res (Phila). 2011;4(3):329-46.
98.Subbaramaiah K, Morris PG, Zhou XK, Morrow M, Du B, Giri D, et al. Increased levels of COX-2 and prostaglandin E2 contribute to elevated aromatase expression in inflamed breast tissue of obese women. Cancer Discov. 2012;2(4):356-65.
99.Cavalieri EL, Rogan EG. Unbalanced metabolism of endogenous estrogens in the etiology and prevention of human cancer. J Steroid Biochem Mol Biol. 2011;125(3-5):169-80.

100. Simpson ER, Clyne C, Rubin G, Boon WC, Robertson K, Britt K, et al. Aromatase--a brief overview. Annu Rev Physiol. 2002;64:93-127.
101. Simpson ER, Brown KA. Obesity and breast cancer: role of inflammation and aromatase. J Mol Endocrinol. 2013;51(3):T51-9.
102. Bowers LW, Brenner AJ, Hursting SD, Tekmal RR, deGraffenried LA. Obesity-associated systemic interleukin-6 promotes pre-adipocyte aromatase expression via increased breast cancer cell prostaglandin E2 production. Breast Cancer Res Treat. 2015;149(1):49-57.
103. McTiernan A, Wu L, Chen C, Chlebowski R, Mossavar-Rahmani Y, Modugno F, et al. Relation of BMI and physical activity to sex hormones in postmenopausal women. Obesity (Silver Spring). 2006;14(9):1662-77.
104. Santen RJ, Brodie H, Simpson ER, Siiteri PK, Brodie A. History of aromatase: saga of an important biological mediator and therapeutic target. Endocr Rev. 2009;30(4):343-75.
105. Ohta M, Kitadai Y, Tanaka S, Yoshihara M, Yasui W, Mukaida N, et al. Monocyte chemoattractant protein-1 expression correlates with macrophage infiltration and tumor vascularity in human gastric carcinomas. Int J Oncol. 2003;22(4):773-8.
106. Solinas G, Germano G, Mantovani A, Allavena P. Tumor-associated macrophages (TAM) as major players of the cancer-related inflammation. J Leukoc Biol. 2009;86(5):1065-73.
107. Murdoch C, Muthana M, Coffelt SB, Lewis CE. The role of myeloid cells in the promotion of tumour angiogenesis. Nat Rev Cancer. 2008;8(8):618-31.
108. Fujimoto H, Sangai T, Ishii G, Ikehara A, Nagashima T, Miyazaki M, et al. Stromal MCP-1 in mammary tumors induces tumor-associated macrophage infiltration and contributes to tumor progression. International Journal of Cancer. 2009;125(6):1276-84.
109. Keeley EC, Mehrad B, Strieter RM. Chemokines as mediators of tumor angiogenesis and neovascularization. Exp Cell Res. 2011;317(5):685-90.
110. Allavena P, Sica A, Solinas G, Porta C, Mantovani A. The inflammatory micro-environment in tumor progression: the role of tumor-associated macrophages. Crit Rev Oncol Hematol. 2008;66(1):1-9.
111. Fang WB, Jokar I, Zou A, Lambert D, Dendukuri P, Cheng N. CCL2/CCR2 chemokine signaling coordinates survival and motility of breast cancer cells through Smad3 protein- and p42/44 mitogen-activated protein kinase (MAPK)-dependent mechanisms. J Biol Chem. 2012;287(43):36593-608.
112. Fang WB, Yao M, Brummer G, Acevedo D, Alhakamy N, Berkland C, et al. Targeted gene silencing of CCL2 inhibits triple negative breast cancer progression by blocking cancer stem cell renewal and M2 macrophage recruitment. Oncotarget. 2016.
113. Saji H, Koike M, Yamori T, Saji S, Seiki M, Matsushima K, et al. Significant correlation of monocyte chemoattractant protein-1 expression with neovascularization and progression of breast carcinoma. Cancer. 2001;92(5):1085-91.
114. Soria G, Ofri-Shahak M, Haas I, Yaal-Hahoshen N, Leider-Trejo L, Leibovich-Rivkin T, et al. Inflammatory mediators in breast cancer: Coordinated expression of TNF alpha & IL-1 beta with CCL2 & CCL5 and effects on epithelial-to-mesenchymal transition. Bmc Cancer. 2011;11.

115. Ueno T, Toi M, Saji H, Muta M, Bando H, Kuroi K, et al. Significance of macrophage chemoattractant protein-1 in macrophage recruitment, angiogenesis, and survival in human breast cancer. Clinical Cancer Research. 2000;6(8):3282-9.
116. Soria G, Yaal-Hahoshen N, Azenshtein E, Shina S, Leider-Trejo L, Ryvo L, et al. Concomitant expression of the chemokines RANTES and MCP-1 in human breast cancer: A basis for tumor-promoting interactions. Cytokine. 2008;44(1):191-200.
117. Valkovic T, Lucin K, Krstulja M, Dobi-Babic R, Jonjic N. Expression of monocyte chemotactic protein-1 in human invasive ductal breast cancer. Pathol Res Pract. 1998;194(5):335-40.
118. Valkovic T, Fuckar D, Stifter S, Matusan K, Hasan M, Dobrila F, et al. Macrophage level is not affected by monocyte chemotactic protein-1 in invasive ductal breast carcinoma. J Cancer Res Clin Oncol. 2005;131(7):453-8.
119. Dwyer RM, Potter-Beirne SM, Harrington KA, Lowery AJ, Hennessy E, Murphy JM, et al. Monocyte chemotactic protein-1 secreted by primary breast tumors stimulates migration of mesenchymal stem cells. Clin Cancer Res. 2007;13(17):5020-7.
120. Goede V, Brogelli L, Ziche M, Augustin HG. Induction of inflammatory angiogenesis by monocyte chemoattractant protein-1. Int J Cancer. 1999;82(5):765-70.
121. Kulbe H, Levinson NR, Balkwill F, Wilson JL. The chemokine network in cancer - much more than directing cell movement. International Journal of Developmental Biology. 2004;48(5-6):489-96.
122. Luboshits G, Shina S, Kaplan O, Engelberg S, Nass D, Lifshitz-Mercer B, et al. Elevated expression of the CC chemokine regulated on activation, normal T cell expressed and secreted (RANTES) in advanced breast carcinoma. Cancer Res. 1999;59(18):4681-7.
123. Lumeng CN, DelProposto JB, Westcott DJ, Saltiel AR. Phenotypic switching of adipose tissue macrophages with obesity is generated by spatiotemporal differences in macrophage subtypes. Diabetes. 2008;57(12):3239-46.
124. Odegaard JI, Ricardo-Gonzalez RR, Goforth MH, Morel CR, Subramanian V, Mukundan L, et al. Macrophage-specific PPARgamma controls alternative activation and improves insulin resistance. Nature. 2007;447(7148):1116-20.
125. Landgraf K, Rockstroh D, Wagner IV, Weise S, Tauscher R, Schwartze JT, et al. Evidence of early alterations in adipose tissue biology and function and its association with obesity-related inflammation and insulin resistance in children. Diabetes. 2015;64(4):1249-61.
126. Bremer AA, Devaraj S, Afify A, Jialal I. Adipose tissue dysregulation in patients with metabolic syndrome. J Clin Endocrinol Metab. 2011;96(11):E1782-8.
127. Arner E, Mejhert N, Kulyte A, Balwierz PJ, Pachkov M, Cormont M, et al. Adipose tissue microRNAs as regulators of CCL2 production in human obesity. Diabetes. 2012;61(8):1986-93.
128. Amano SU, Cohen JL, Vangala P, Tencerova M, Nicoloro SM, Yawe JC, et al. Local proliferation of macrophages contributes to obesity-associated adipose tissue inflammation. Cell Metab. 2014;19(1):162-71.
129. Kamei N, Tobe K, Suzuki R, Ohsugi M, Watanabe T, Kubota N, et al. Overexpression of monocyte chemoattractant protein-1 in adipose tissues causes macrophage recruitment and insulin resistance. J Biol Chem. 2006;281(36):26602-14.

130. Inouye KE, Shi H, Howard JK, Daly CH, Lord GM, Rollins BJ, et al. Absence of CC chemokine ligand 2 does not limit obesity-associated infiltration of macrophages into adipose tissue. Diabetes. 2007;56(9):2242-50.
131. Galastri S, Zamara E, Milani S, Novo E, Provenzano A, Delogu W, et al. Lack of CC chemokine ligand 2 differentially affects inflammation and fibrosis according to the genetic background in a murine model of steatohepatitis. Clin Sci (Lond). 2012;123(7):459-71.
132. Enos RT, Velazquez KT, Murphy EA. Insight into the impact of dietary saturated fat on tissue-specific cellular processes underlying obesity-related diseases. J Nutr Biochem. 2014;25(6):600-12.
133. Grotto D, Zied E. The Standard American Diet and its relationship to the health status of Americans. Nutrition in clinical practice : official publication of the American Society for Parenteral and Enteral Nutrition. 2010;25(6):603-12.
134. Matthews DR, Hosker JP, Rudenski AS, Naylor BA, Treacher DF, Turner RC. Homeostasis model assessment: insulin resistance and beta-cell function from fasting plasma glucose and insulin concentrations in man. Diabetologia. 1985;28(7):412-9.
135. Schneider CA, Rasband WS, Eliceiri KW. NIH Image to ImageJ: 25 years of image analysis. Nature methods. 2012;9(7):671-5.
136. Bradford MM. A rapid and sensitive method for the quantitation of microgram quantities of protein utilizing the principle of protein-dye binding. Analytical biochemistry. 1976;72:248-54.
137. Enos RT, Velazquez KT, McClellan JL, Cranford TL, Walla MD, Murphy EA. Reducing the dietary omega-6:omega-3 utilizing alpha-linolenic acid; not a sufficient therapy for attenuating high-fat-diet-induced obesity development nor related detrimental metabolic and adipose tissue inflammatory outcomes. PLoS One. 2014;9(4):e94897.
138. Enos RT, Velazquez KT, McClellan JL, Cranford TL, Walla MD, Murphy EA. Lowering the dietary omega-6: omega-3 does not hinder nonalcoholic fatty-liver disease development in a murine model. Nutr Res. 2015;35(5):449-59.
139. Kim DH, Gutierrez-Aguilar R, Kim HJ, Woods SC, Seeley RJ. Increased adipose tissue hypoxia and capacity for angiogenesis and inflammation in young diet-sensitive C57 mice compared with diet-resistant FVB mice. International journal of obesity. 2013;37(6):853-60.
140. Le Lay S, Boucher J, Rey A, Castan-Laurell I, Krief S, Ferre P, et al. Decreased resistin expression in mice with different sensitivities to a high-fat diet. Biochemical and biophysical research communications. 2001;289(2):564-7.
141. Hu CC, Qing K, Chen Y. Diet-induced changes in stearoyl-CoA desaturase 1 expression in obesity-prone and -resistant mice. Obesity research. 2004;12(8):1264-70.
142. Montgomery MK, Hallahan NL, Brown SH, Liu M, Mitchell TW, Cooney GJ, et al. Mouse strain-dependent variation in obesity and glucose homeostasis in response to high-fat feeding. Diabetologia. 2013;56(5):1129-39.
143. Anantha S. Metlakunta MS, Abhiram Sahu. Hypothalamic Phosphatidylinositol 3-Kinase Pathway of Leptin Signaling Is Impaired during the development of Diet-Induced Obesity in FVB/N mice. Endocrinology. 2008;149(3):1121-8.
144. Kanda H, Tateya S, Tamori Y, Kotani K, Hiasa K, Kitazawa R, et al. MCP-1 contributes to macrophage infiltration into adipose tissue, insulin resistance, and hepatic steatosis in obesity. The Journal of clinical investigation. 2006;116(6):1494-505.

145. Weisberg SP, Hunter D, Huber R, Lemieux J, Slaymaker S, Vaddi K, et al. CCR2 modulates inflammatory and metabolic effects of high-fat feeding. The Journal of clinical investigation. 2006;116(1):115-24.
146. Chow FY, Nikolic-Paterson DJ, Ma FY, Ozols E, Rollins BJ, Tesch GH. Monocyte chemoattractant protein-1-induced tissue inflammation is critical for the development of renal injury but not type 2 diabetes in obese db/db mice. Diabetologia. 2007;50(2):471-80.
147. Chen A, Mumick S, Zhang C, Lamb J, Dai H, Weingarth D, et al. Diet induction of monocyte chemoattractant protein-1 and its impact on obesity. Obesity research. 2005;13(8):1311-20.
148. Kirk EA, Sagawa ZK, McDonald TO, O'Brien KD, Heinecke JW. Monocyte chemoattractant protein deficiency fails to restrain macrophage infiltration into adipose tissue [corrected]. Diabetes. 2008;57(5):1254-61.
149. Zimmermann HW, Tacke F. Modification of chemokine pathways and immune cell infiltration as a novel therapeutic approach in liver inflammation and fibrosis. Inflamm Allergy Drug Targets. 2011;10(6):509-36.
150. Younce C, Kolattukudy P. MCP-1 induced protein promotes adipogenesis via oxidative stress, endoplasmic reticulum stress and autophagy. Cell Physiol Biochem. 2012;30(2):307-20.
151. Group USCSW. United States Cancer Statistics: 1999-2012 Incidence and Mortality Web-based Report. Department of Health and Human Services, Centers for Disease Control and Prevention, and National Cancer Institute; 2015.
152. Society AC. Learn about cancer: Breast Cancer 2016 [updated 05/04/2016. Available from: http://www.cancer.org/cancer/breastcancer/detailedguide/breast-cancer-key-statistics.
153. Haffty BG, Yang Q, Reiss M, Kearney T, Higgins SA, Weidhaas J, et al. Locoregional relapse and distant metastasis in conservatively managed triple negative early-stage breast cancer. J Clin Oncol. 2006;24(36):5652-7.
154. Dolle JM, Daling JR, White E, Brinton LA, Doody DR, Porter PL, et al. Risk factors for triple-negative breast cancer in women under the age of 45 years. Cancer Epidemiol Biomarkers Prev. 2009;18(4):1157-66.
155. Dent R, Trudeau M, Pritchard KI, Hanna WM, Kahn HK, Sawka CA, et al. Triple-negative breast cancer: clinical features and patterns of recurrence. Clin Cancer Res. 2007;13(15 Pt 1):4429-34.
156. Harris LN, Broadwater G, Lin NU, Miron A, Schnitt SJ, Cowan D, et al. Molecular subtypes of breast cancer in relation to paclitaxel response and outcomes in women with metastatic disease: results from CALGB 9342. Breast Cancer Res. 2006;8(6):R66.
157. Badve S, Dabbs DJ, Schnitt SJ, Baehner FL, Decker T, Eusebi V, et al. Basal-like and triple-negative breast cancers: a critical review with an emphasis on the implications for pathologists and oncologists. Mod Pathol. 2011;24(2):157-67.
158. Tischkowitz M, Brunet JS, Begin LR, Huntsman DG, Cheang MC, Akslen LA, et al. Use of immunohistochemical markers can refine prognosis in triple negative breast cancer. BMC Cancer. 2007;7:134.
159. Rodler E, Korde L, Gralow J. Current treatment options in triple negative breast cancer. Breast Dis. 2010;32(1-2):99-122.

160. Bennett CN, Green JE. Genomic analyses as a guide to target identification and preclinical testing of mouse models of breast cancer. Toxicol Pathol.38(1):88-95.
161. Maroulakou IG, Anver M, Garrett L, Green JE. Prostate and mammary adenocarcinoma in transgenic mice carrying a rat C3(1) simian virus 40 large tumor antigen fusion gene. Proc Natl Acad Sci U S A. 1994;91(23):11236-40.
162. Green JE, Shibata MA, Yoshidome K, Liu ML, Jorcyk C, Anver MR, et al. The C3(1)/SV40 T-antigen transgenic mouse model of mammary cancer: ductal epithelial cell targeting with multistage progression to carcinoma. Oncogene. 2000;19(8):1020-7.
163. Steiner J, Davis J, McClellan J, Enos R, Carson J, Fayad R, et al. Dose-dependent benefits of quercetin on tumorigenesis in the C3(1)/SV40Tag transgenic mouse model of breast cancer. Cancer Biol Ther. 2014;15(11):1456-67.
164. Warden CH, Fisler JS. Comparisons of diets used in animal models of high-fat feeding. Cell Metab. 2008;7(4):277.
165. Velazquez KT, Enos RT, McClellan JL, Cranford TL, Chatzistamou I, Singh UP, et al. MicroRNA-155 deletion promotes tumorigenesis in the azoxymethane-dextran sulfate sodium model of colon cancer. Am J Physiol Gastrointest Liver Physiol. 2016;310(6):G347-58.
166. Hoenerhoff MJ, Shibata MA, Bode A, Green JE. Pathologic progression of mammary carcinomas in a C3(1)/SV40 T/t-antigen transgenic rat model of human triple-negative and Her2-positive breast cancer. Transgenic Res. 2011;20(2):247-59.
167. Balkwill FR, Mantovani A. Cancer-related inflammation: common themes and therapeutic opportunities. Semin Cancer Biol. 2012;22(1):33-40.
168. Balkwill F. Cancer and the chemokine network. Nat Rev Cancer. 2004;4(7):540-50.
169. Bailey C, Negus R, Morris A, Ziprin P, Goldin R, Allavena P, et al. Chemokine expression is associated with the accumulation of tumour associated macrophages (TAMs) and progression in human colorectal cancer. Clin Exp Metastasis. 2007;24(2):121-30.
170. McClellan JL, Davis JM, Steiner JL, Enos RT, Jung SH, Carson JA, et al. Linking tumor-associated macrophages, inflammation, and intestinal tumorigenesis: role of MCP-1. Am J Physiol Gastrointest Liver Physiol. 2012;303(10):G1087-95.
171. Fridlender ZG, Buchlis G, Kapoor V, Cheng G, Sun J, Singhal S, et al. CCL2 blockade augments cancer immunotherapy. Cancer Res. 2010;70(1):109-18.
172. Soria G, Yaal-Hahoshen N, Azenshtein E, Shina S, Leider-Trejo L, Ryvo L, et al. Concomitant expression of the chemokines RANTES and MCP-1 in human breast cancer: a basis for tumor-promoting interactions. Cytokine. 2008;44(1):191-200.
173. Yao M, Yu E, Staggs V, Fan F, Cheng N. Elevated expression of chemokine C-C ligand 2 in stroma is associated with recurrent basal-like breast cancers. Mod Pathol. 2016;29(8):810-23.
174. Qian BZ, Li J, Zhang H, Kitamura T, Zhang J, Campion LR, et al. CCL2 recruits inflammatory monocytes to facilitate breast-tumour metastasis. Nature. 2011;475(7355):222-5.
175. Hollmen M, Roudnicky F, Karaman S, Detmar M. Characterization of macrophage--cancer cell crosstalk in estrogen receptor positive and triple-negative breast cancer. Sci Rep. 2015;5:9188.

176. Su S, Liu Q, Chen J, Chen J, Chen F, He C, et al. A positive feedback loop between mesenchymal-like cancer cells and macrophages is essential to breast cancer metastasis. Cancer Cell. 2014;25(5):605-20.
177. Patsialou A, Wyckoff J, Wang Y, Goswami S, Stanley ER, Condeelis JS. Invasion of human breast cancer cells in vivo requires both paracrine and autocrine loops involving the colony-stimulating factor-1 receptor. Cancer Res. 2009;69(24):9498-506.
178. Soria G, Ben-Baruch A. The inflammatory chemokines CCL2 and CCL5 in breast cancer. Cancer Lett. 2008;267(2):271-85.
179. Mantovani A, Allavena P, Sica A, Balkwill F. Cancer-related inflammation. Nature. 2008;454(7203):436-44.
180. Gautier EL, Shay T, Miller J, Greter M, Jakubzick C, Ivanov S, et al. Gene-expression profiles and transcriptional regulatory pathways that underlie the identity and diversity of mouse tissue macrophages. Nat Immunol. 2012;13(11):1118-28.
181. Nguyen KQ, Tsou WI, Calarese DA, Kimani SG, Singh S, Hsieh S, et al. Overexpression of MERTK receptor tyrosine kinase in epithelial cancer cells drives efferocytosis in a gain-of-function capacity. J Biol Chem. 2014;289(37):25737-49.
182. Knupfer H, Preiss R. Significance of interleukin-6 (IL-6) in breast cancer (review). Breast Cancer Res Treat. 2007;102(2):129-35.
183. Salgado R, Junius S, Benoy I, Van Dam P, Vermeulen P, Van Marck E, et al. Circulating interleukin-6 predicts survival in patients with metastatic breast cancer. Int J Cancer. 2003;103(5):642-6.
184. Wolin KY, Carson K, Colditz GA. Obesity and cancer. Oncologist. 2010;15(6):556-65.
185. Simpson ER, Brown KA. Minireview: Obesity and breast cancer: a tale of inflammation and dysregulated metabolism. Mol Endocrinol.27(5):715-25.
186. Nunez NP, Perkins SN, Smith NC, Berrigan D, Berendes DM, Varticovski L, et al. Obesity accelerates mouse mammary tumor growth in the absence of ovarian hormones. Nutr Cancer. 2008;60(4):534-41.
187. Nkhata KJ, Ray A, Dogan S, Grande JP, Cleary MP. Mammary tumor development from T47-D human breast cancer cells in obese ovariectomized mice with and without estradiol supplements. Breast Cancer Res Treat. 2009;114(1):71-83.
188. Ray A, Nkhata KJ, Grande JP, Cleary MP. Diet-induced obesity and mammary tumor development in relation to estrogen receptor status. Cancer Lett. 2007;253(2):291-300.
189. Cleary MP, Hu X, Grossmann ME, Juneja SC, Dogan S, Grande JP, et al. Prevention of mammary tumorigenesis by intermittent caloric restriction: does caloric intake during refeeding modulate the response? Exp Biol Med (Maywood). 2007;232(1):70-80.
190. Krishnan K, Bassett JK, Macinnis RJ, English DR, Hopper JL, McLean CA, et al. Associations between weight in early adulthood, change in weight and breast cancer risk in postmenopausal women. Cancer Epidemiol Biomarkers Prev.
191. Lin EY, Jones JG, Li P, Zhu L, Whitney KD, Muller WJ, et al. Progression to malignancy in the polyoma middle T oncoprotein mouse breast cancer model provides a reliable model for human diseases. Am J Pathol. 2003;163(5):2113-26.
192. Biotek O. EZNA Total RNA Kit II Manual 2015 [Available from: http://omegabiotek.com/store/wp-content/uploads/2013/09/R6934-Total-RNA-Kit-II-Combo-Online1.pdf.

193. Bocchinfuso WP, Korach KS. Mammary gland development and tumorigenesis in estrogen receptor knockout mice. J Mammary Gland Biol Neoplasia. 1997;2(4):323-34.

# APPENDIX A

## PERMISSION TO REPRINT